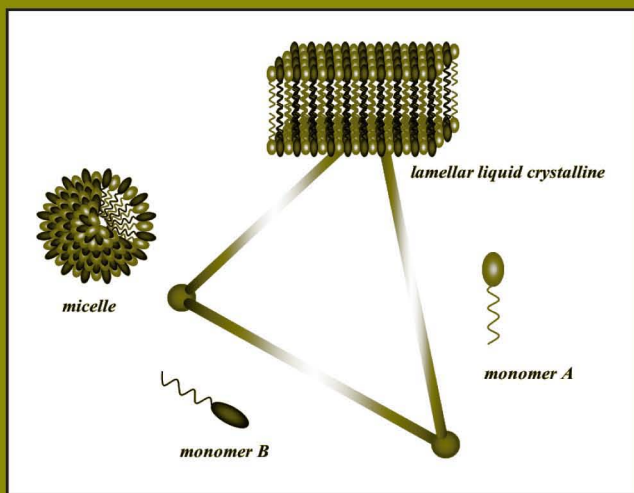


surfactant science series

volume **124**

MIXED SURFACTANT SYSTEMS

Second Edition,
Revised and Expanded



edited by

Masahiko Abe

John F. Scamehorn

MIXED SURFACTANT SYSTEMS

SURFACTANT SCIENCE SERIES

FOUNDING EDITOR

MARTIN J. SCHICK

1918–1998

SERIES EDITOR

ARTHUR T. HUBBARD

*Santa Barbara Science Project
Santa Barbara, California*

ADVISORY BOARD

DANIEL BLANKSCHTEIN

*Department of Chemical
Engineering
Massachusetts Institute of
Technology
Cambridge, Massachusetts*

S. KARABORNI

*Shell International Petroleum
Company Limited
London, England*

LISA B. QUENCER

*The Dow Chemical Company
Midland, Michigan*

JOHN F. SCAMEHORN

*Institute for Applied Surfactant
Research
University of Oklahoma
Norman, Oklahoma*

P. SOMASUNDARAN

*Henry Krumb School of Mines
Columbia University
New York, New York*

ERIC W. KALER

*Department of Chemical
Engineering
University of Delaware
Newark, Delaware*

CLARENCE MILLER

*Department of Chemical
Engineering
Rice University
Houston, Texas*

DON RUBINGH

*The Procter & Gamble Company
Cincinnati, Ohio*

BEREND SMIT

*Shell International Oil Products
B.V.
Amsterdam, The Netherlands*

JOHN TEXTER

*Strider Research Corporation
Rochester, New York*

1. Nonionic Surfactants, *edited by Martin J. Schick* (see also Volumes 19, 23, and 60)
2. Solvent Properties of Surfactant Solutions, *edited by Kozo Shinoda* (see Volume 55)
3. Surfactant Biodegradation, *R. D. Swisher* (see Volume 18)
4. Cationic Surfactants, *edited by Eric Jungermann* (see also Volumes 34, 37, and 53)
5. Detergency: Theory and Test Methods (in three parts), *edited by W. G. Cutler and R. C. Davis* (see also Volume 20)
6. Emulsions and Emulsion Technology (in three parts), *edited by Kenneth J. Lissant*
7. Anionic Surfactants (in two parts), *edited by Warner M. Linfield* (see Volume 56)
8. Anionic Surfactants: Chemical Analysis, *edited by John Cross*
9. Stabilization of Colloidal Dispersions by Polymer Adsorption, *Tatsuo Sato and Richard Ruch*
10. Anionic Surfactants: Biochemistry, Toxicology, Dermatology, *edited by Christian Gloxhuber* (see Volume 43)
11. Anionic Surfactants: Physical Chemistry of Surfactant Action, *edited by E. H. Lucassen-Reynders*
12. Amphoteric Surfactants, *edited by B. R. Bluestein and Clifford L. Hilton* (see Volume 59)
13. Demulsification: Industrial Applications, *Kenneth J. Lissant*
14. Surfactants in Textile Processing, *Arved Datyner*
15. Electrical Phenomena at Interfaces: Fundamentals, Measurements, and Applications, *edited by Ayao Kitahara and Akira Watanabe*
16. Surfactants in Cosmetics, *edited by Martin M. Rieger* (see Volume 68)
17. Interfacial Phenomena: Equilibrium and Dynamic Effects, *Clarence A. Miller and P. Neogi*
18. Surfactant Biodegradation: Second Edition, Revised and Expanded, *R. D. Swisher*
19. Nonionic Surfactants: Chemical Analysis, *edited by John Cross*
20. Detergency: Theory and Technology, *edited by W. Gale Cutler and Erik Kissa*
21. Interfacial Phenomena in Apolar Media, *edited by Hans-Friedrich Eicke and Geoffrey D. Parfitt*
22. Surfactant Solutions: New Methods of Investigation, *edited by Raoul Zana*
23. Nonionic Surfactants: Physical Chemistry, *edited by Martin J. Schick*
24. Microemulsion Systems, *edited by Henri L. Rosano and Marc Clausee*

25. Biosurfactants and Biotechnology, *edited by Naim Kosaric, W. L. Cairns, and Neil C. C. Gray*
26. Surfactants in Emerging Technologies, *edited by Milton J. Rosen*
27. Reagents in Mineral Technology, *edited by P. Somasundaran and Brij M. Moudgil*
28. Surfactants in Chemical/Process Engineering, *edited by Darsh T. Wasan, Martin E. Ginn, and Dinesh O. Shah*
29. Thin Liquid Films, *edited by I. B. Ivanov*
30. Microemulsions and Related Systems: Formulation, Solvency, and Physical Properties, *edited by Maurice Bourrel and Robert S. Schechter*
31. Crystallization and Polymorphism of Fats and Fatty Acids, *edited by Nissim Garti and Kiyotaka Sato*
32. Interfacial Phenomena in Coal Technology, *edited by Gregory D. Botsaris and Yuli M. Glazman*
33. Surfactant-Based Separation Processes, *edited by John F. Scamehorn and Jeffrey H. Harwell*
34. Cationic Surfactants: Organic Chemistry, *edited by James M. Richmond*
35. Alkylene Oxides and Their Polymers, *F. E. Bailey, Jr., and Joseph V. Koleske*
36. Interfacial Phenomena in Petroleum Recovery, *edited by Norman R. Morrow*
37. Cationic Surfactants: Physical Chemistry, *edited by Donn N. Rubingh and Paul M. Holland*
38. Kinetics and Catalysis in Microheterogeneous Systems, *edited by M. Grätzel and K. Kalyanasundaram*
39. Interfacial Phenomena in Biological Systems, *edited by Max Bender*
40. Analysis of Surfactants, *Thomas M. Schmitt* (see Volume 96)
41. Light Scattering by Liquid Surfaces and Complementary Techniques, *edited by Dominique Langevin*
42. Polymeric Surfactants, *Irja Piirma*
43. Anionic Surfactants: Biochemistry, Toxicology, Dermatology. Second Edition, Revised and Expanded, *edited by Christian Gloxhuber and Klaus Künstler*
44. Organized Solutions: Surfactants in Science and Technology, *edited by Stig E. Friberg and Björn Lindman*
45. Defoaming: Theory and Industrial Applications, *edited by P. R. Garrett*
46. Mixed Surfactant Systems, *edited by Keizo Ogino and Masahiko Abe*
47. Coagulation and Flocculation: Theory and Applications, *edited by Bohuslav Dobiás*

48. Biosurfactants: Production Properties Applications, edited by Naim Kosaric
49. Wettability, *edited by John C. Berg*
50. Fluorinated Surfactants: Synthesis Properties Applications, *Erik Kissa*
51. Surface and Colloid Chemistry in Advanced Ceramics Processing, *edited by Robert J. Pugh and Lennart Bergström*
52. Technological Applications of Dispersions, *edited by Robert B. McKay*
53. Cationic Surfactants: Analytical and Biological Evaluation, *edited by John Cross and Edward J. Singer*
54. Surfactants in Agrochemicals, *Tharwat F. Tadros*
55. Solubilization in Surfactant Aggregates, *edited by Sherril D. Christian and John F. Scamehorn*
56. Anionic Surfactants: Organic Chemistry, *edited by Helmut W. Stache*
57. Foams: Theory, Measurements, and Applications, *edited by Robert K. Prud'homme and Saad A. Khan*
58. The Preparation of Dispersions in Liquids, *H. N. Stein*
59. Amphoteric Surfactants: Second Edition, *edited by Eric G. Lomax*
60. Nonionic Surfactants: Polyoxyalkylene Block Copolymers, *edited by Vaughn M. Nace*
61. Emulsions and Emulsion Stability, *edited by Johan Sjöblom*
62. Vesicles, *edited by Morton Rosoff*
63. Applied Surface Thermodynamics, *edited by A. W. Neumann and Jan K. Spelt*
64. Surfactants in Solution, *edited by Arun K. Chattopadhyay and K. L. Mittal*
65. Detergents in the Environment, *edited by Milan Johann Schwuger*
66. Industrial Applications of Microemulsions, *edited by Conxita Solans and Hironobu Kunieda*
67. Liquid Detergents, *edited by Kuo-Yann Lai*
68. Surfactants in Cosmetics: Second Edition, Revised and Expanded, *edited by Martin M. Rieger and Linda D. Rhein*
69. Enzymes in Detergency, *edited by Jan H. van Ee, Onno Misset, and Erik J. Baas*
70. Structure-Performance Relationships in Surfactants, *edited by Kunio Esumi and Minoru Ueno*
71. Powdered Detergents, *edited by Michael S. Showell*
72. Nonionic Surfactants: Organic Chemistry, *edited by Nico M. van Os*
73. Anionic Surfactants: Analytical Chemistry, Second Edition, Revised and Expanded, *edited by John Cross*

74. Novel Surfactants: Preparation, Applications, and Biodegradability, *edited by Kristier Holmberg*
75. Biopolymers at Interfaces, *edited by Martin Malmsten*
76. Electrical Phenomena at Interfaces: Fundamentals, Measurements, and Applications, Second Edition, Revised and Expanded, *edited by Hiroyuki Ohshima and Kunio Furusawa*
77. Polymer-Surfactant Systems, *edited by Jan C. T. Kwak*
78. Surfaces of Nanoparticles and Porous Materials, *edited by James A. Schwarz and Cristian I. Contescu*
79. Surface Chemistry and Electrochemistry of Membranes, *edited by Torben Smith Sørensen*
80. Interfacial Phenomena in Chromatography, *edited by Emile Pefferkorn*
81. Solid-Liquid Dispersions, *Bohuslav Dobiáš, Xueping Qiu, and Wolfgang von Rybinski*
82. Handbook of Detergents, *editor in chief: Uri Zoller*
Part A: Properties, *edited by Guy Broze*
83. Modern Characterization Methods of Surfactant Systems, *edited by Bernard P. Binks*
84. Dispersions: Characterization, Testing, and Measurement, *Erik Kissa*
85. Interfacial Forces and Fields: Theory and Applications, *edited by Jyh-Ping Hsu*
86. Silicone Surfactants, *edited by Randal M. Hill*
87. Surface Characterization Methods: Principles, Techniques, and Applications, *edited by Andrew J. Milling*
88. Interfacial Dynamics, *edited by Nikola Kallay*
89. Computational Methods in Surface and Colloid Science, *edited by Malgorzata Borówko*
90. Adsorption on Silica Surfaces, *edited by Eugène Papirer*
91. Nonionic Surfactants: Alkyl Polyglucosides, *edited by Dieter Balzer and Harald Lüders*
92. Fine Particles: Synthesis, Characterization, and Mechanisms of Growth, *edited by Tadao Sugimoto*
93. Thermal Behavior of Dispersed Systems, *edited by Nissim Garti*
94. Surface Characteristics of Fibers and Textiles, *edited by Christopher M. Pastore and Paul Kiekens*
95. Liquid Interfaces in Chemical, Biological, and Pharmaceutical Applications, *edited by Alexander G. Volkov*
96. Analysis of Surfactants: Second Edition, Revised and Expanded, *Thomas M. Schmitt*
97. Fluorinated Surfactants and Repellents: Second Edition, Revised and Expanded, *Erik Kissa*
98. Detergency of Specialty Surfactants, *edited by Floyd E. Friedli*

99. Physical Chemistry of Polyelectrolytes, *edited by Tsetska Radeva*
100. Reactions and Synthesis in Surfactant Systems, *edited by John Texter*
101. Protein-Based Surfactants: Synthesis, Physicochemical Properties, and Applications, *edited by Ifendu A. Nnanna and Jiding Xia*
102. Chemical Properties of Material Surfaces, *Marek Kosmulski*
103. Oxide Surfaces, *edited by James A. Wingrave*
104. Polymers in Particulate Systems: Properties and Applications, *edited by Vincent A. Hackley, P. Somasundaran, and Jennifer A. Lewis*
105. Colloid and Surface Properties of Clays and Related Minerals, *Rossmann F. Giese and Carel J. van Oss*
106. Interfacial Electrokinetics and Electrophoresis, *edited by Ángel V. Delgado*
107. Adsorption: Theory, Modeling, and Analysis, *edited by József Tóth*
108. Interfacial Applications in Environmental Engineering, *edited by Mark A. Keane*
109. Adsorption and Aggregation of Surfactants in Solution, *edited by K. L. Mittal and Dinesh O. Shah*
110. Biopolymers at Interfaces: Second Edition, Revised and Expanded, *edited by Martin Malmsten*
111. Biomolecular Films: Design, Function, and Applications, *edited by James F. Rusling*
112. Structure–Performance Relationships in Surfactants: Second Edition, Revised and Expanded, *edited by Kunio Esumi and Minoru Ueno*
113. Liquid Interfacial Systems: Oscillations and Instability, *Rudolph V. Birkh, Vladimir A. Briskman, Manuel G. Velarde, and Jean-Claude Legros*
114. Novel Surfactants: Preparation, Applications, and Biodegradability: Second Edition, Revised and Expanded, *edited by Krister Holmberg*
115. Colloidal Polymers: Synthesis and Characterization, *edited by Abdelhamid Elaissari*
116. Colloidal Biomolecules, Biomaterials, and Biomedical Applications, *edited by Abdelhamid Elaissari*
117. Gemini Surfactants: Synthesis, Interfacial and Solution-Phase Behavior, and Applications, *edited by Raoul Zana and Jiding Xia*
118. Colloidal Science of Flotation, *Anh V. Nguyen and Hans Joachim Schulze*
119. Surface and Interfacial Tension: Measurement, Theory, and Applications, *edited by Stanley Hartland*

120. Microporous Media: Synthesis, Properties, and Modeling,
Freddy Romm
121. Handbook of Detergents, *editor in chief: Uri Zoller*
Part B: Environmental Impact, *edited by Uri Zoller*
122. Luminous Chemical Vapor Deposition and Interface Engineering,
Hirotsugu Yasuda
123. Handbook of Detergents, *editor in chief: Uri Zoller*
Part C: Analysis, *edited by Heinrich Waldhoff*
and Rüdiger Spilker
124. Mixed Surfactant Systems: Second Edition, Revised
and Expanded, *edited by Masahiko Abe and John F. Scamehorn*

ADDITIONAL VOLUMES IN PREPARATION

MIXED SURFACTANT SYSTEMS

**Second Edition,
Revised and Expanded**

edited by

Masahiko Abe

*Faculty of Science and Technology
and Institute of Colloid and Interface Science
Tokyo University of Science
Chiba, Japan*

John F. Scamehorn

*Institute for Applied Surfactant Research
University of Oklahoma
Norman, Oklahoma, U.S.A.*



MARCEL DEKKER

NEW YORK

CRC Press
Taylor & Francis Group
6000 Broken Sound Parkway NW, Suite 300
Boca Raton, FL 33487-2742

© 2004 by Taylor & Francis Group, LLC
CRC Press is an imprint of Taylor & Francis Group, an Informa business

No claim to original U.S. Government works
Version Date: 20141027

International Standard Book Number-13: 978-1-4200-3101-0 (eBook - PDF)

This book contains information obtained from authentic and highly regarded sources. Reasonable efforts have been made to publish reliable data and information, but the author and publisher cannot assume responsibility for the validity of all materials or the consequences of their use. The authors and publishers have attempted to trace the copyright holders of all material reproduced in this publication and apologize to copyright holders if permission to publish in this form has not been obtained. If any copyright material has not been acknowledged please write and let us know so we may rectify in any future reprint.

Except as permitted under U.S. Copyright Law, no part of this book may be reprinted, reproduced, transmitted, or utilized in any form by any electronic, mechanical, or other means, now known or hereafter invented, including photocopying, microfilming, and recording, or in any information storage or retrieval system, without written permission from the publishers.

For permission to photocopy or use material electronically from this work, please access www.copyright.com (<http://www.copyright.com/>) or contact the Copyright Clearance Center, Inc. (CCC), 222 Rosewood Drive, Danvers, MA 01923, 978-750-8400. CCC is a not-for-profit organization that provides licenses and registration for a variety of users. For organizations that have been granted a photocopy license by the CCC, a separate system of payment has been arranged.

Trademark Notice: Product or corporate names may be trademarks or registered trademarks, and are used only for identification and explanation without intent to infringe.

Visit the Taylor & Francis Web site at
<http://www.taylorandfrancis.com>

and the CRC Press Web site at
<http://www.crcpress.com>



Sherril D. Christian (1931–2000)

Dedicated to the memory of Sherril D. Christian, George Lynn Cross Professor of Chemistry at the University of Oklahoma. Sherril was a solution thermodynamicist, who spent the last twenty years of his career studying the fundamentals and applications of surfactants. He had the highest standards as scientist and educator and was a good friend.

Preface

It has been known for a long time that surfactant mixtures can exhibit substantially different properties than single surfactants. Papers on this topic have been published in the scientific literature for at least half a century. Practical applications utilizing these mixture synergisms are widespread and new uses continue to be found.

As far as we know, the first book dedicated to surfactant mixtures was published in 1986 (Scamehorn, J.F. (Editor), *Phenomena in Mixed Surfactant Systems*, ACS Symp. Ser., Vol. 311). In 1992, a second book appeared (Rubingh, D.N., and Holland, P.M. (Editors), *Mixed Surfactant Systems*, ACS Symp. Ser., Vol. 501). Finally, in 1993, the first edition of this book was published as Volume 46 of the Marcel Dekker Surfactant Science Series (Ogino, K., and Abe, M. (Editors), *Mixed Surfactant Systems*, Marcel Dekker, New York).

The current editors organized a session at PACIFICHEM held in Hawaii in December, 2000 and this second edition of *Mixed Surfactant Systems* evolved from that symposium. With the retirement of Professor Ogino, Professor Abe became senior

editor and he asked Professor Scamehorn to become co-editor. In editing the book, we replaced about two thirds of the contributors in the first edition, avoided overlap of subjects with those in the first edition except where progress merited an updated chapter, and attempted to incorporate the results of the newest experimental and theoretical investigations on mixed surfactant systems as much as possible. Thus, the book contains a variety of topics including monolayers of mixed surfactants, diffusion of mixed micelles, mixed micelles of fluorinated surfactants, mixed micelles of conventional surfactants and biosurfactants, sponge-like vesicles of mixed surfactants, admicelles of mixed surfactants, liquid crystals of mixed surfactants, mixed micelles of stimulus-responsive surfactants, mixtures of surfactants and polymers, photolysis of mixed surfactants, and new measurement methods and techniques.

We earnestly hope that this book will help the reader appreciate the rapid progress made in understanding surfactant mixtures and to help them make unique inventions using mixed surfactant systems.

Masahiko Abe
John F. Scamehorn

Contents

<i>Preface</i>	<i>v</i>
<i>Contributors</i>	<i>xi</i>
1. Miscibility in Binary Mixtures of Surfactants <i>Makoto Aratono and Takanori Takiue</i>	1
2. Micro-Phase Separation in Two-Dimensional Amphiphile Systems <i>Teiji Kato and Ken-Ichi Iimura</i>	59
3. The Differential Conductivity Technique and Its Application to Mixed Surfactant Solutions for Determining Ionic Constants <i>Masahiro Manabe</i>	93
4. Diffusion Processes in Mixed Surfactant Systems <i>Toshihiro Tominaga</i>	135

5. Mixed Micellar Aggregates of Nonionic Surfactants with Short Hydrophobic Tails 165
Vincenzo Vitagliano, Gerardino D'Errico, Ornella Ortona, and Luigi Paduano
6. The Effect of Mixed Counterions on the Micelle Structure of Perfluorinated Anionic Surfactants 205
Dobrin Petrov Bossev, Mutsuo Matsumoto, and Masaru Nakahara
7. Delayed Degradation of Drugs by Mixed Micellization with Biosurfactants 229
Shoko Yokoyama
8. A Thermodynamic Study on Competitive or Selective Solubilization of 1:1 Mixed Solubilizate Systems: Solubilization of Different Sterols Mixtures by Bile Salt Micelles in Water 257
Shigemi Nagadome and Gohsuke Sugihara
9. Phase Behavior and Microstructure in Aqueous Mixtures of Cationic and Anionic Surfactants 289
Eric W. Kaler, Kathi L. Herrington, Daniel J. Iampietro, Bret A. Coldren, Hee-Tae Jung, and Joseph A. Zasadzinski
10. Phase Behavior and Microstructure of Liquid Crystals in Mixed Surfactant Systems 339
Carlos Rodriguez and Hironobu Kunieda
11. Sponge Structures of Amphiphiles in Solution 375
Kazuhiro Fukada and Kazuo Tajima
12. Surfactant Gels from Small Unilamellar Vesicles 403
M. Müller and H. Hoffmann

13. Microscopic Phase Separation in Mixed Micellar Solutions <i>Shigeyoshi Miyagishi, Tsuyoshi Asakawa, and Akio Ohta</i>	431
14. Dynamic Interfacial Properties of Mixed Surfactant Systems Containing Light-Sensitive Surfactants <i>Jason Y. Shin and Nicholas L. Abbott</i>	477
15. Control of Molecular Aggregate Formation and Solubilization Using Electro- and Photoresponsive Surfactant Mixtures <i>Hideki Sakai and Masahiko Abe</i>	507
16. Adsolubilization by Binary Surfactant Mixtures <i>Kunio Esumi</i>	545
17. Admicellization and Adsolubilization of Fluorocarbon–Hydrocarbon Mixed Chain Surfactant <i>Masahiko Abe and Hideki Sakai</i>	573
18. Precipitation of Surfactant Mixtures <i>John F. Scamehorn and Jeffrey H. Harwell</i>	601
19. Surfactant–Polymer Interactions <i>Marina Tsianou and Paschalis Alexandridis</i>	657
20. Ultrasonic Relaxation Studies of Mixed Surfactant Systems—Analysis of Data to Yield Kinetic Parameters <i>T. Thurn, D. M. Bloor, and E. Wyn-Jones</i>	709
21. Photocatalysis at Solid/Liquid Interfaces—Photooxidation of Mixed Aqueous Surfactants at the $\text{TiO}_2/\text{H}_2\text{O}$ Interface <i>H. Hidaka, M. S. Vohra, N. Watanabe, and N. Serpone</i>	769
<i>Index</i>	795

Contributors

Nicholas L. Abbott Department of Chemical and Biological Engineering, University of Wisconsin, Madison, Wisconsin, U.S.A.

Masahiko Abe Faculty of Science and Technology and Institute of Colloid and Interface Science, Tokyo University of Science, Chiba, Japan

Paschalis Alexandridis Department of Chemical and Biological Engineering, University at Buffalo, The State University of New York, Buffalo, New York, U.S.A.

Makoto Aratono Kyushu University, Hakozaki, Fukuoka, Japan

Tsuyoshi Asakawa Kanazawa University, Kanazawa, Japan

D. M. Bloor School of Sciences, Chemistry, University of Salford, Salford, United Kingdom

Dobrin Petrov Bossev National Institute of Standards and Technology, Gaithersburg, Maryland, U.S.A.

Bret A. Coldren Advanced Encapsulation, Santa Barbara, California, U.S.A.

Gerardino D'Errico Dipartimento di Chimica, Università di Napoli "Federico II", Complesso di Monte S. Angelo, Napoli, Italy

Kunio Esumi Department of Applied Chemistry and Institute of Colloid and Interface Science, Tokyo University of Science, Tokyo, Japan

Kazuhiro Fukada Department of Biochemistry and Food Science, Faculty of Agriculture, Kagawa University, Kagawa, Japan

Jeffrey H. Harwell Institute for Applied Surfactant Research, University of Oklahoma, Norman, Oklahoma

Kathi L. Herrington W. L. Gore and Associates, Newark, Delaware, U.S.A.

H. Hidaka Frontier Research Center for the Global Environment Protection, Meisei University, Tokyo, Japan

H. Hoffmann University of Bayreuth, Physical Chemistry I, Bayreuth, Germany

Daniel J. Iampietro Merck and Company, Rahway, New Jersey, U.S.A.

Ken-Ichi Iimura Faculty of Engineering, Utsunomiya University, Utsunomiya, Japan

Hee-Tae Jung Department of Chemical and Biomolecular Engineering, Korea Advanced Institute of Science and Technology, Daejeon, Korea

Eric W. Kaler Department of Chemical Engineering, University of Delaware, Newark, Delaware, U.S.A.

Teiji Kato Faculty of Engineering, Utsunomiya University, Utsunomiya, Japan

Hironobu Kunieda Graduate School of Engineering, Yokohama National University, Yokohama, Japan

Masahiro Manabe Niihama National College of Technology,
Niihama, Ehime, Japan

Mutsuo Matsumoto Institute for Chemical Research, Kyoto
University, Kyoto, Japan

Shigeyoshi Miyagishi Kanazawa University, Kanazawa,
Japan

M. Müller University of Bayreuth, Physical Chemistry I,
Bayreuth, Germany

Shigemi Nagadome Department of Chemistry, Fukuoka
University, Fukuoka, Japan

Masaru Nakahara Institute for Chemical Research, Kyoto
University, Kyoto, Japan

Akio Ohta Kanazawa University, Kanazawa, Japan

Ornella Ortona Dipartimento di Chimica, Università di
Napoli “Federico II”, Complesso di Monte S. Angelo, Napoli,
Italy

Luigi Paduano Dipartimento di Chimica, Università di Napoli
“Federico II”, Complesso di Monte S. Angelo, Napoli, Italy

Carlos Rodriguez Graduate School of Engineering,
Yokohama National University, Yokohama, Japan

Hideki Sakai Faculty of Science and Technology and Insti-
tute of Colloid and Interface Science, Tokyo University of
Science, Chiba, Japan

John F. Scamehorn Institute for Applied Surfactant
Research, University of Oklahoma, Norman, Oklahoma

N. Serpone Department of Chemistry and Biochemistry,
Concordia University, Montreal (Quebec), Canada

Jason Y. Shin Department of Chemical and Biological
Engineering, University of Wisconsin, Madison, Wisconsin,
U.S.A.

Gohsuke Sugihara Department of Chemistry, Fukuoka
University, Fukuoka, Japan

Kazuo Tajima Department of Chemistry, and Hightech Research Center, Faculty of Engineering, Kanagawa University, Kanagawa, Japan

Takanori Takiue Kyushu University, Hakozaki, Fukuoka, Japan

T. Thurn School of Sciences, Chemistry, University of Salford, Salford, United Kingdom

Toshihiro Tominaga Department of Applied Chemistry, Okayama University of Science, Okayama, Japan

Marina Tsianou Department of Chemical and Biological Engineering, University at Buffalo, The State University of New York, Buffalo, New York, U.S.A.

Vincenzo Vitagliano Dipartimento di Chimica, Università di Napoli "Federico II", Complesso di Monte S. Angelo, Napoli, Italy

M. S. Vohra Frontier Research Center for the Global Environment Protection, Meisei University, Tokyo, Japan

N. Watanabe Frontier Research Center for the Global Environment Protection, Meisei University, Tokyo, Japan

E. Wyn-Jones School of Sciences, Chemistry, University of Salford, Salford, United Kingdom

Shoko Yokoyama School of Pharmaceutical Sciences, Kyushu University of Health and Welfare, Miyazaki, Japan

Joseph A. Zasadzinski Department of Chemical Engineering and Materials, University of California, Santa Barbara, California, U.S.A.

Miscibility in Binary Mixtures of Surfactants

MAKOTO ARATONO and TAKANORI TAKIUE

Kyushu University, Hakozaki, Fukuoka, Japan

SYNOPSIS

The miscibility in binary mixtures of surfactants in the organized assemblies at the interface and in the solution is summarized on the basis of the phase diagrams of adsorption, micelle formation, and vesicle formation. In Section II, the thermodynamic equations to obtain the phase diagrams are given for some combinations of binary surfactant systems. Furthermore the criterion of an ideal mixing is proposed. In Section III, the miscibility in the adsorbed film and micelle is demonstrated for some representative systems by using the phase diagrams and the excess Gibbs free energy. In Section IV,

the vesicle–micelle transition in the aqueous mixture and the phase transition in the adsorbed films at the oil/water interface are shown and examined from the viewpoint of the miscibility of the surfactants.

I. INTRODUCTION

The adsorption and micelle formation of surfactant mixtures have been studied extensively, not only by various experimental techniques, but also by theoretical considerations. In this decade several experimental techniques have been developed such as the scattering and reflection of X-rays and neutrons, electron microscopy, probe microscopy, imaging techniques, and so on. They and their developments have been introduced and reviewed in the literature [1,2]. By means of these techniques, many researchers have inquired deeply into the structures of interfaces, adsorbed films, micelles, and vesicles and their dependencies on the composition of surfactants in the bulk solution. At the same time, theoretical considerations have been improved from the one-parameter model of Rubingh *et al.* [3] and molecular thermodynamics have also been developed steadily, especially by Blankschtein *et al.* [4,5]. The theoretical aspects of micellization of surfactant mixtures have been reviewed very recently by Hines [6], in which the more rigorous and refined theoretical developments have been updated.

In our previous reviews on miscibility in binary mixtures of surfactant [7], the miscibilities of surfactants in the adsorbed films and micellar states have been considered by developing the thermodynamic equations for constructing the phase diagrams of adsorption and micelle formation and then by examining the phase diagrams closely. During the course, newly defined compositions of surfactants in the adsorbed film and micelle were introduced to take a dissociation of ionic surfactants into account explicitly and could describe the miscibility very adequately from the thermodynamic viewpoint: its usefulness was examined and proved in the cases of nonionic–nonionic, ionic–ionic, and nonionic–ionic surfactant mixtures.

Although the review here is basically a further extension of our previous reviews from a theoretical point of view, the criteria of an ideal mixing in the adsorbed film and micelle are newly and definitely proposed for some types of surfactant mixtures. The nonideal mixing is then expressed quantitatively either in the activity coefficients or in the excess Gibbs free energy of adsorption and micelle formation. Furthermore, the spontaneous vesicle formation of anionic-cationic surfactant mixtures, and then the vesicle-micelle transition, are introduced on the basis of our thermodynamic strategy [8]. Other new topics in this review are the phase transition of adsorbed films of the long chain hydrocarbon and fluorocarbon alcohol mixtures at the oil/water interface and the relationship between the miscibility and the phase transition of the adsorbed films [9,10].

II. THERMODYNAMIC EQUATIONS

To evaluate the composition of surfactants in the adsorbed film thermodynamically, it is indispensable that the surface tension of their aqueous solution/air interface is measured as a function of the two concentrations of the two surfactants at a given temperature and pressure. Among some combinations of the two concentration variables, the combination of the total concentration of the surfactants and the mole fraction of one surfactant is most useful to evaluate directly the composition of surfactant in the adsorbed film from the surface tension results [7,11]. For a nonionic surfactant mixture, the total concentration and the mole fraction are defined unequivocally. For a mixture comprising at least one ionic surfactant, however, the dissociation of ionic surfactants should be taken into account in their definition and thus there are some different ways to define them. Therefore, it is convenient to employ the most suitable concentration variables as the case may be and then describe the total differential of the surface tension as a function of them. A thorough derivation of the basic expression of the total differential of surface tension is given in our previous studies from this perspective [7]. Then only the very

key points of the thermodynamic equations are demonstrated here. Furthermore, although the dependencies of the surface tension on temperature and pressure afford information on the entropy and volume changes associated with the adsorption, let us leave out this topic for want of space.

In the following, thermodynamic equations for a binary ionic surfactant mixture without common ions (Section II.A) are summarized from our previous papers [11], because the equations are most general in their form. The analogues for a binary ionic surfactant mixture with common ions (Section II.B) are slightly different from those of the Section II.A, but essentially the same. For ionic–nonionic (Section II.C) and nonionic–nonionic (Section II.D) surfactant mixtures, the analogues are apparently quite the same as the equations of Section II.A.

A. Ionic and Ionic Surfactant Mixtures Without Common Ions

Let us first consider the adsorption from an aqueous solution of a binary ionic surfactant mixture without common ions at their aqueous solution/air interface. Surfactants 1 and 2 are assumed to be strong electrolytes and dissociate into $\nu_{1,a}$ a ions and $\nu_{1,c}$ c ions, and $\nu_{2,b}$ b ions and $\nu_{2,d}$ d ions, respectively. Then the total differential of the surface tension γ is written as

$$d\gamma = -\Gamma_a d\mu_a - \Gamma_c d\mu_c - \Gamma_b d\mu_b - \Gamma_d d\mu_d \quad (1)$$

at constant temperature and pressure, where the electroneutrality conditions of surfactants in the bulk solution are already taken into account and Γ_i is the surface excess concentration of ion i according to the two dividing planes method [12]. By assuming the aqueous solutions are ideally dilute, the surface tension γ is expressed as a function of the total molality of the ions m and the mole fraction of the second surfactant in the bulk solution X_2 as

$$d\gamma = -(RT\Gamma/m) dm - (RT\Gamma/X_1X_2)(Y_2 - X_2) dX_2 \quad (2)$$

Here m and X_2 are defined by

$$\begin{aligned} m &= m_a + m_c + m_b + m_d \\ &= \nu_1 m_1 + \nu_2 m_2 \end{aligned} \quad (3)$$

and

$$\begin{aligned} X_2 &= (m_b + m_d)/m \\ &= \nu_2 m_2/m \end{aligned} \quad (4)$$

respectively. Here ν_1 and ν_2 are the number of ions dissociated from surfactants 1 and 2 defined as

$$\nu_1 = \nu_{1,a} + \nu_{1,c} \quad (5)$$

and

$$\nu_2 = \nu_{2,b} + \nu_{2,d} \quad (6)$$

The mole fraction of the second surfactant in the adsorbed film Y_2 is analogously defined in terms of the surface excess concentrations of the ions as

$$Y_2 = (\Gamma_b + \Gamma_d)/\Gamma \quad (7)$$

where Γ is the total surface excess concentration of ions given by

$$\Gamma = \Gamma_a + \Gamma_c + \Gamma_b + \Gamma_d \quad (8)$$

The theoretical background of why these definitions are appropriate is pointed out in our previous studies [7,11].

Then, from Eq. (2), the mole fraction Y_2 is evaluated by applying the equation

$$Y_2 = X_2 - (X_1 X_2/m)(\partial m/\partial X_2)_{T,p,\gamma} \quad (9)$$

to the m vs X_2 curve at a given surface tension. Plotting the m vs X_2 curve together with the m vs Y_2 curve, we have a diagram expressing the quantitative relation between the mole fractions of the two states, that is the bulk solution and the adsorbed

films. We call this the phase diagram of adsorption (PDA) at the given surface tension.

To inquire more deeply into the miscibility of surfactant molecules, it is advantageous to examine the deviation of the Y_2 values from the corresponding values of the ideal mixing Y_2^{id} and then evaluate the activity coefficients of the surfactant in the adsorbed film. For this purpose, we have to derive the expression for Y_2^{id} and then know how to estimate the activity coefficients. This is performed by deriving the thermodynamic relations for the equilibrium between the adsorbed film and the aqueous solution at a given surface tension. In principle, the equilibrium condition is that the electrochemical potentials of ions in the bulk solution are equal to those in the adsorbed film. However, since the concentration of an ion cannot be changed individually without changing its counter ion concentration, it is convenient to introduce the mean chemical potential of the surfactant i in the bulk solution μ_i and that in the adsorbed film ζ_i of the binary surfactant mixture. For the first surfactant, these are defined by

$$\mu_1 = (v_{1,a}\tilde{\mu}_a + v_{1,c}\tilde{\mu}_c)/v_1 \quad (10)$$

and

$$\zeta_1 = (v_{1,a}\tilde{\zeta}_a + v_{1,c}\tilde{\zeta}_c)/v_1 \quad (11)$$

respectively. Here $\tilde{\mu}_j$ and $\tilde{\zeta}_j$ are the electrochemical potentials of ion j . Similarly, introducing the mean chemical potential μ_i^0 and the molality m_i^0 of the pure surfactant i at the given surface tension, μ_i can be expressed as [11]

$$\mu_i = \mu_i^0 + RT \ln X_i m/m_i^0 \quad (12)$$

Here the solution is assumed to be ideally dilute as shown in Eq. (1).

Even when the bulk solution is ideally dilute, the preferential adsorption of counter ions to the pair surfactant ions, i.e., $\Gamma_a/v_{1a} \neq \Gamma_c/v_{1c}$ and $\Gamma_b/v_{2b} \neq \Gamma_d/v_{2d}$, often comes about and then the ions do not mix ideally in the adsorbed film.

From this point of view, the definition of the mean chemical potentials ζ_i is rather complicated. Even in those cases, however, it has been proved that ζ_i is written in a similar form to Eq. (12) as

$$\zeta_i = \zeta_i^0 + RT \ln f_i^H Y_i \quad (13)$$

where ζ_i^0 is the mean chemical potential of the pure surfactant i at the given γ [11]. Here it should be noted that f_i^H is the mean activity coefficient of the surfactant i and becomes unity neither when the preferential adsorption takes place nor when the interaction among species in the mixed-surfactant system is different from that in the pure surfactant system. Therefore f_i^H can elucidate quantitatively nonideal mixing of surfactants in the adsorbed film in terms of preferential adsorption and interaction between ions [11].

Now substituting the mean chemical potentials into the equilibrium conditions between the bulk solution and the adsorbed film given by

$$\mu_i = \zeta_i \quad (14)$$

and using the equilibrium condition for the pure surfactant i at the same γ given by

$$\mu_i^0 = \zeta_i^0 \quad (15)$$

we yield the equation describing the equilibrium relationship among the bulk concentration, the mole fractions in the bulk solution and the surface, and the activity coefficient

$$X_i m / m_i^0 = f_i^H Y_i \quad (16)$$

Therefore, f_i^H is evaluated from the surface tension measurements since the quantities on the left-hand sides of Eq. (16) are obtained from the γ vs m curve at different X_2 , and Y_i is evaluated by using Eq. (9) at a given surface tension. Once f_i^H is evaluated, the excess Gibbs free energy of adsorption per mole of surfactant mixture g^{HE} is calculated according to

the equation

$$g^{\text{HE}} = RT(Y_1 \ln f_1^{\text{H}} + Y_2 \ln f_2^{\text{H}}) \quad (17)$$

The nonideal mixing of surfactants in the adsorbed film is recognized from the shape of the PDA as follows. Since $f_i^{\text{H}} = 1$ corresponds to the ideal mixing, Eq. (16) for the first and second surfactants with $f_i^{\text{H}} = 1$ provides the criterion of the ideal mixing as the straight line connecting the molality values of the pure surfactants at the given surface tension

$$m = m_1^0 + (m_2^0 - m_1^0)Y_2 \quad (18)$$

Here it should be emphasized again that the dissociation of surfactants into ions are explicitly taken into account in the definition of m , m_i^0 , and Y_2 as given by Eqs (3) and (7).

Now let us turn to the micelle formation of surfactant mixtures. We have shown that the micelle formation is described by the analogous equations to those describing the adsorption by using the excess molar thermodynamic quantities of mixed micelle [13,14]. The analogue of Eq. (2) is given by

$$(RT/C) dC = -(RT/X_1X_2)(Z_2 - X_2) dX_2 \quad (19)$$

Here C is the total molality of ions at the critical micelle concentration (CMC) defined by Eq. (3) and Z_2 is the mole fraction of the second surfactant in the micelle particles defined in terms of the excess number of ions N_i by

$$Z_2 = (N_b + N_d)/N \quad (20)$$

where N is the total excess number of ions given by

$$N = N_a + N_c + N_b + N_d \quad (21)$$

Then the mole fraction Z_2 is estimated from the C vs X_2 curves by using the equation

$$Z_2 = X_2 - (X_1X_2/C)(\partial C/\partial X_2)_{T,p} \quad (22)$$

Furthermore the equilibrium relationship among the bulk monomer concentration C and the mole fractions of the surfactant i in their monomeric state X_i and that in the micelle particles Z_i , and the activity coefficients in the micelle f_i^M at the CMC are expressed by using the total molality at the CMC of the pure surfactant i , C_i^0 , as

$$X_i C / C_i^0 = f_i^M Z_i \quad (23)$$

Therefore the excess Gibbs free energy of micelle formation per mole of surfactant mixture g^{ME} and the criterion of the ideal mixing in the micelle on the phase diagram of micelle formation (PDM) are respectively given by

$$g^{ME} = RT(Z_1 \ln f_1^M + Z_2 \ln f_2^M) \quad (24)$$

and

$$C = C_1^0 + (C_2^0 - C_1^0) Z_2 \quad (25)$$

At the concentrations above the CMC, micelle particles in solution are in equilibrium with the adsorbed film. Using Eqs (2) and (19), we have the equation

$$Y_2^C = Z_2 - (X_1 X_2 / RT \Gamma^C) (\partial \gamma^C / \partial X_2)_{T,p} \quad (26)$$

Then the relation between the mole fractions of the micelle Z_2 and adsorbed film Y_2^C at the CMC can be examined from the change of the surface tension at the CMC γ^C with X_2 .

B. Ionic and Ionic Surfactant Mixtures with Common Ions

Let us consider that ion c is common to the two surfactants: surfactant 1 dissociates into $v_{1,a}$ a ions and $v_{1,c}$ c ions and surfactant 2 into $v_{2,b}$ b ions and $v_{2,c}$ c ions, respectively. Taking account of this dissociation, the total differential of γ is given by

$$d\gamma = -\Gamma_a d\mu_a - \Gamma_c d\mu_c - \Gamma_b d\mu_b \quad (27)$$

The mole fraction of surfactant 2, Y_2 , in the adsorbed film is reasonably defined as the ratio of the total excess concentration of ions originated from surfactant 2 to the total excess concentration of all the ions Γ by

$$\begin{aligned} Y_2 &= (\nu_{2,b}\Gamma_2 + \nu_{2,c}\Gamma_2)/\Gamma \\ &= \nu_2\Gamma_2/\Gamma \end{aligned} \quad (28)$$

where

$$\Gamma = \Gamma_a + \Gamma_c + \Gamma_b = \nu_{1,a}\Gamma_1 + \nu_{1,c}\Gamma_1 + \nu_{2,c}\Gamma_2 + \nu_{2,b}\Gamma_2 \quad (29)$$

In this case, it has been shown that Eq. (2) is transformed into

$$d\gamma = -(RT\Gamma/m)dm - \Phi(\nu)(RT\Gamma/X_1X_2)(Y_2 - X_2) dX_2 \quad (30)$$

where $\Phi(\nu)$ are defined by

$$\Phi(\nu) = 1 - (\nu_{1,c}/\nu_1)(\nu_{2,c}/\nu_2)/[(\nu_{1,c}/\nu_1)X_1 + (\nu_{2,c}/\nu_2)X_2] \quad (31)$$

Then the mole fraction Y_2 is evaluated by using the equation

$$Y_2 = X_2 - (X_1X_2/m)(\partial m/\partial X_2)_{T,p,\nu}/\Phi(\nu) \quad (32)$$

The analogue of Eq. (16) is derived by following the same process as shown in Section II.A, but the resulting equation is found to be a rather complicated form [11]. Let us then take up a special case of $\nu_{1,c}/\nu_1 = \nu_{2,c}/\nu_2$, being of most frequent occurrence. In this case, we have the relation

$$X_i^{1/\nu} m/m_i^0 = f_i^H Y_i^{1/\nu} \quad (33)$$

and then the activity coefficient f_i^H and the excess Gibbs free energy of adsorption defined by Eq. (17) are calculated. Now the ideal mixing in the adsorbed film is obtained by putting $f_i^H = 1$ in Eq. (33) as

$$m^\nu = (m_1^0)^\nu + [(m_2^0)^\nu - (m_1^0)^\nu]Y_2 \quad (34)$$

where we put $1/\nu = \nu_{1,c}/\nu_1 = \nu_{2,c}/\nu_2$. Comparing Eq. (34) to Eq. (18), we note the large difference between them: the criterion of the ideal mixing for a binary mixture with common ions is not the straight line connecting m_1^0 and m_2^0 , but the one connecting $(m_1^0)^\nu$ and $(m_2^0)^\nu$ at the given surface tension.

Also for the micelle formation, the mole fraction in the mixed micelle Z_2 is evaluated by

$$Z_2 = X_2 - (X_1 X_2 / C) (\partial C / \partial X_2)_{T,p} / \Phi(\nu) \quad (35)$$

Furthermore the activity coefficient in the micelle is calculated from the equation

$$X_i^{1/\nu} C / C_i^0 = f_i^M Z_i^{1/\nu} \quad (36)$$

The relation between C and Z_2 for the ideal mixing on PDM is given by

$$C^\nu = (C_1^0)^\nu + [(C_2^0)^\nu - (C_1^0)^\nu] Z_2 \quad (37)$$

for the mixtures of $1/\nu = \nu_{1,c}/\nu_1 = \nu_{2,c}/\nu_2$.

C. Ionic and Nonionic Surfactant Mixture

Let us consider a mixture in which surfactant 1 is ionic and dissociates into $\nu_{1,a} a$ ions and $\nu_{1,c} c$ ions and surfactant 2 is nonionic. The total differential of γ is written as

$$d\gamma = -\Gamma_a d\mu_a - \Gamma_c d\mu_c - \Gamma_2 d\mu_2 \quad (38)$$

Introducing m , X_2 , Γ , and Y_2 defined by

$$\begin{aligned} m &= m_a + m_c + m_2, & X_2 &= m_2/m, \\ \Gamma &= \Gamma_a + \Gamma_c + \Gamma_2, & Y_2 &= \Gamma_2/\Gamma \end{aligned} \quad (39)$$

we obtain the same equation as Eq. (2) in its apparent form. Furthermore, introducing the analogous definitions to Eqs (39) for N and Z_2 by

$$N = N_a + N_c + N_2, \quad Z_2 = N_2/N \quad (40)$$

for the mixed micelle formation, we also have the same equation as Eq. (22) in its apparent form. Therefore the equations derived for Section II.A are also applicable in this section. However it should be noted that m , X_2 , Γ , Y_2 , N , and Z_2 are defined differently in each case.

D. Nonionic and Nonionic Surfactant Mixture

The total differential of γ is simply written as

$$d\gamma = -\Gamma_1 d\mu_1 - \Gamma_2 d\mu_2 \quad (41)$$

Also in this case we obtain the same equation as Eq. (2) in its apparent form with the following definitions

$$m = m_1 + m_2, \quad X_2 = m_2/m, \quad \Gamma = \Gamma_1 + \Gamma_2, \quad Y_2 = \Gamma_2/\Gamma \quad (42)$$

For the mixed micelle formation, we also have the same equation as Eq. (22) with the definitions given by

$$N = N_1 + N_2, \quad Z_2 = N_2/N \quad (43)$$

Therefore the equations derived for Section II.A. are again applicable to this section.

III. ADSORPTION AND MICELLE FORMATION

A. Nonionic–Nonionic Surfactant Mixtures

The mixtures of analogues of nonionic surfactants often show ideal mixing in the adsorbed films and micelle when the length of hydrocarbon chains is not very different from each other [15–18]. However, even in these cases, the compositions in the adsorbed film and micelle are different from that in the bulk solution. Here we show two cases of nonionic surfactant mixture. The first one is the very typical nonionic surfactant mixture: the mixture of pentaethyleneglycol monodecyl ether (C10E5) and pentaethyleneglycol monooctyl ether (C8E5). The second one is the hydrocarbon and fluorocarbon surfactant mixture: the mixture of tetraethyleneglycol monodecyl ether (C10E4) and tetraethyleneglycol mono-1,1,7-trihydrododecafluoroheptyl ether (FC7E4). The former is expected to be

ideally and the latter nonideally mixed in their adsorbed films and micelles [19].

1. Pentaethyleneglycol Monodecyl Ether (C10E5)–Pentaethyleneglycol Monooctyl Ether (C8E5)

The surface tension γ is shown as a function of the total molality m at constant mole fraction of C8E5 X_2 defined by Eq. (42) (Fig. 1) [20]. The shape of the curves change very regularly with X_2 and the molality at the CMC C was determined unambiguously from the break points of the curves. The mole fraction of C8E5 in the adsorbed film Y_2 was evaluated by applying Eq. (9) to the m vs X_2 curves at a given surface tension and plotted as the m vs Y_2 curves together with the corresponding m vs X_2 curves in Fig. 2. Figure 2 gives the PDA at different surface tensions. The C values are plotted against X_2 and the mole fraction of C8E5 in the micelle Z_2 calculated by applying Eq. (22) to the C vs X_2 curve are also plotted in Fig. 3. Figure 3 is the PDM at the CMC.

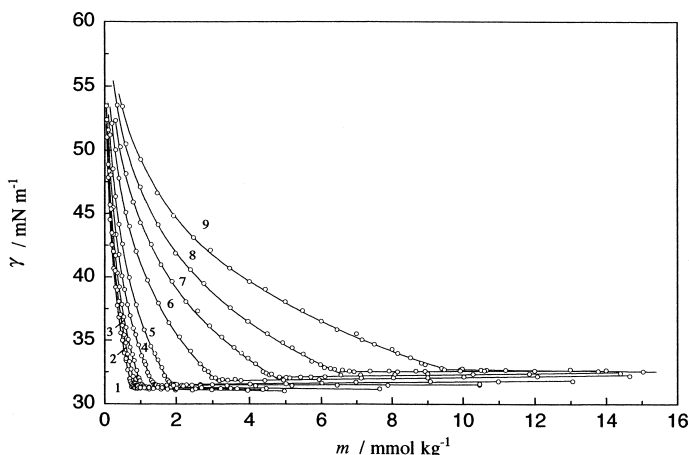


Figure 1 Surface tension vs total molality curves of the C10E5–C8E5 system at constant mole fraction: (1) $X_2=0$ (C10E5), (2) 0.1273, (3) 0.2777, (4) 0.4801, (5) 0.6389, (6) 0.8200, (7) 0.9117, (8) 0.9596, (9) 1 (C8E5).

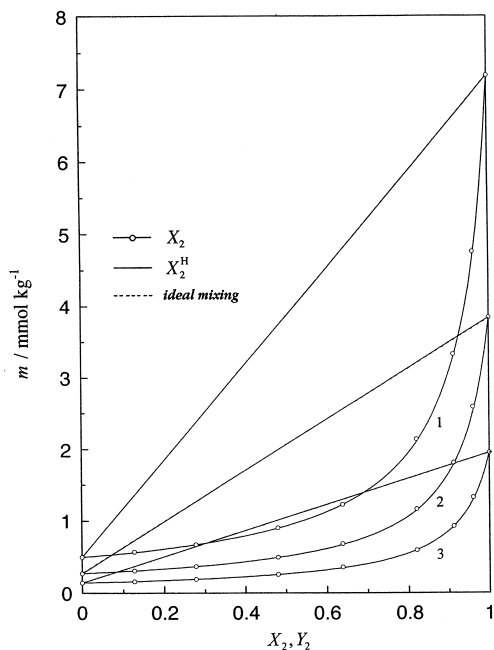


Figure 2 Phase diagram of adsorption of the C10E5–C8E5 system: (1) $\gamma = 35 \text{ mN m}^{-1}$, (2) 40, (3) 45.

The PDAs and PDM manifest that the adsorbed films and the micelle are richer in C10E5 molecules, being more surface active and having lower CMC, than the bulk solution. Furthermore we note the linear m vs Y_2 and C vs Z_2 relations. Thus it is realized that C10E5 and C8E5 molecules are mixed ideally in the adsorbed film and micelle on the basis of Eqs (18) and (25). The C10E5–C8E4 mixture shows the ideal mixing in the adsorbed film but the positive deviation from the ideal mixing in the micelle [20].

2. Tetraethyleneglycol Monodecyl Ether (C10E4)–Tetraethyleneglycol Mono-1,1,7-trihydrododecafluoroheptyl Ether (FC7E4)

It is well known that very weak interactions between hydrocarbon and fluorocarbon chains of surfactants often

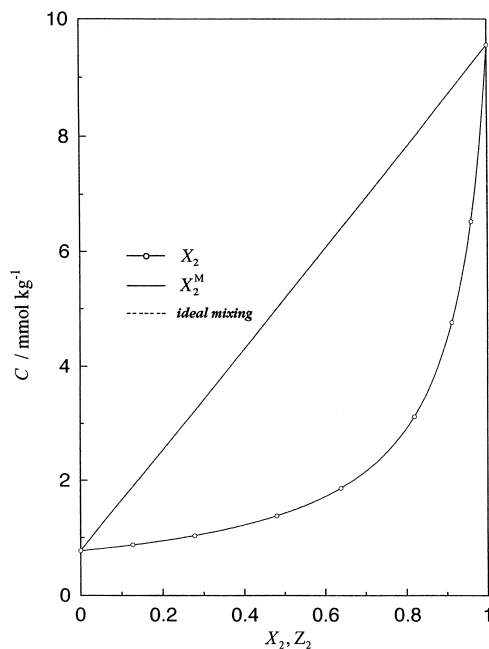


Figure 3 Phase diagram of micelle formation of the C10E5–C8E5 system.

give rise to de-mixing of the surfactants or its tendency in the adsorbed films and micelle [19,21]. However, there are only a few studies on the nonionic hydrocarbon and fluorocarbon surfactant mixtures [22]. Here we demonstrate the miscibility of fluorinated surfactant FC7E4 in the adsorbed film and micelle with hydrogenated C10E4 [23]. The latter was chosen because its surface activity is very similar to that of the former.

The γ vs m curves at constant X_2 are shown in Fig. 4. Although all the curves appear to sit very closely to each other at concentrations below the CMC, the m value at a given surface tension changes very regularly with X_2 as is shown clearly by solid lines in Fig. 5. The m values increase with the other component added and reach a maximum. Applying Eq. (9) to the solid lines, we evaluated the mole fraction of FC7E4 in the adsorbed film Y_2 (broken lines) and constructed the PDAs in Fig. 5. It is noticeable that the m vs Y_2 curves deviate positively from the ideal mixing line given by Eq. (18)

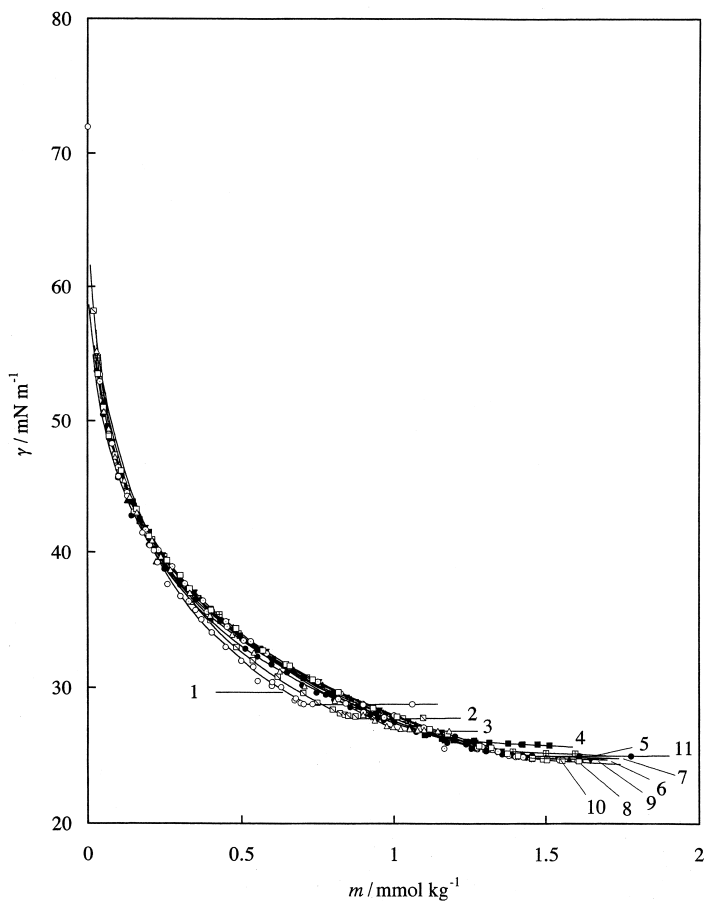


Figure 4 Surface tension vs total molality curves of the C10E4–FC7E4 system at constant mole fraction: (1) $X_2=0$ (C10E4), (2) 0.190, (3) 0.366, (4) 0.500, (5) 0.622, (6) 0.701, (7) 0.750, (8) 0.780, (9) 0.801, (10) 0.900, (11) 1 (FC7E4).

and always sit outside the m vs X_2 curves with the coincidence at the maximum point as expected from Eq. (9). Thus the PDA is azeotropic.

The positively azeotropic miscibility mainly comes from the weak interaction between the hydrocarbon and fluorocarbon chains. This is estimated quantitatively by the activity coefficients in the adsorbed films f_i^H and then the excess Gibbs free energy g^{HE} given by Eqs (16) and (17), respectively.

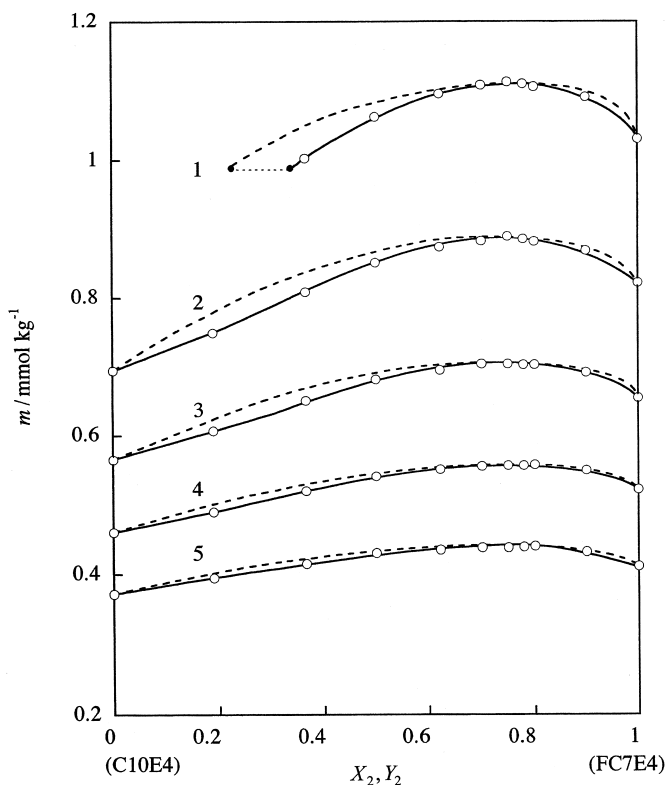


Figure 5 Phase diagram of adsorption of the C10E4–FC7E4 system: (1) $\gamma = 27 \text{ mN m}^{-1}$, (2) 29, (3) 31, (4) 33, (5) 35; (—) m vs X_2 , (·····) m vs Y_2 .

The g^{HE} values are plotted against the mole fraction in the adsorbed films at various surface tensions in Fig. 6. The positive values of g^{HE} suggest that the interaction between C10E4 and FC7E4 molecules is less attractive than that between the same species alone. This is also substantiated by the positive excess area per adsorbed molecule A^{HE} , which was evaluated by applying the equation

$$A^{\text{HE}} = -(1/N_A)(\partial g^{\text{HE}}/\partial \gamma)_{T,p,Y_2} \quad (44)$$

to the dependence of g^{HE} on the surface tension shown in Fig. 6.

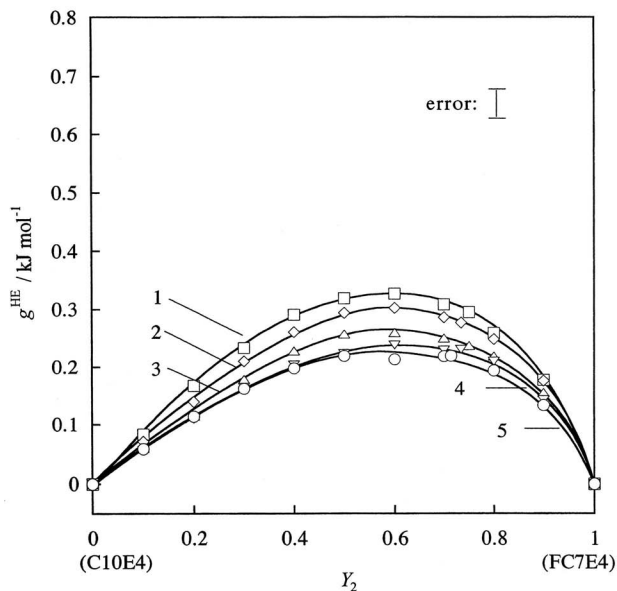


Figure 6 Excess Gibbs free energy of adsorption vs mole fraction in the adsorbed film curves of the C10E4-FC7E4 system: (1) $\gamma = 29 \text{ mN m}^{-1}$, (2) 31, (3) 33, (4) 35, (5) 37.

The PDM demonstrates more clearly the less attractive interaction between C10E4 and FC7E4 molecules. Figure 7 is the PDM and reveals the positive azeotropy that the addition of one component to the other increases the CMC with each other. Furthermore, in Fig. 8 the excess Gibbs free energy of micelle formation g^{ME} is compared to that of adsorption at the CMC $g^{\text{HE,C}}$. The values of the latter are smaller than those of the former. The existence of the difference between g^{ME} and $g^{\text{HE,C}}$ reveals the nonideal mixing and the large difference is attributable to the different molecular orientations in the adsorbed film and the micelle; the hydrophobic chains are expected to be closer to each other in the micelle than in the adsorbed film.

B. Nonionic-Ionic Surfactant Mixtures

Ionic-nonionic surfactant systems have been investigated for different kinds of surfactant mixtures and exhibit the strong

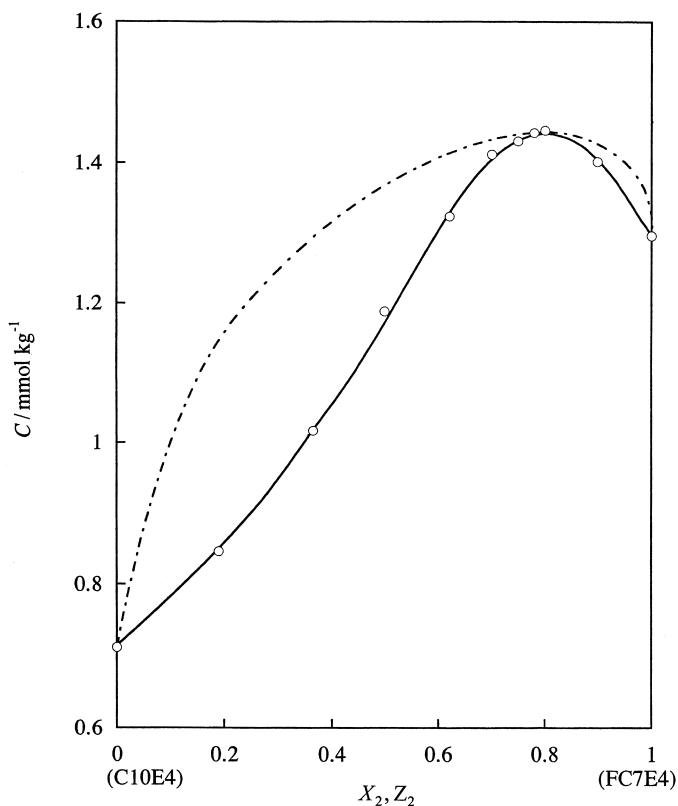


Figure 7 Phase diagram of micelle formation of the C10E4–FC7E4 system : (—) C vs X_2 , (·····) C vs Z_2 .

interaction between different species both in the adsorbed films and in micelle [24–29]. However, there exist several controversies and uncertainties on the type, magnitude, and mechanism of the interaction. Here we demonstrate the strong interaction observed in the anionic–nonionic and cationic–nonionic mixtures: sodium dodecyl sulfate (SDS)–tetraethyleneglycol monoethyl ether (C8E4) [29] and dodecylammonium chloride (DAC)–C8E4 systems [27]. From the results of the two mixtures, we propose a probable physical picture of these strong interactions on the basis of the thermodynamic quantities obtained.

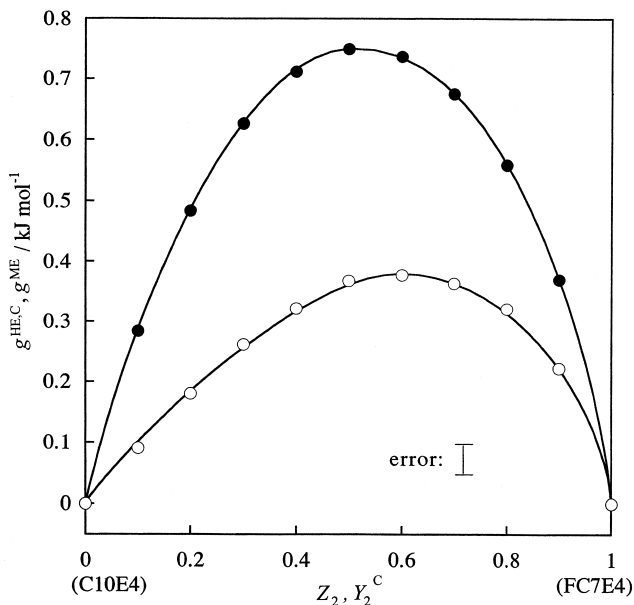


Figure 8 Excess Gibbs free energy of adsorption and micelle formation vs mole fraction curves of the C10E4–FC7E4 system: (●) $g^{HE,C}$ vs Y_2^C , (○) g^{ME} vs Z_2 .

1. Sodium Dodecyl Sulfate (SDS)–Tetraethylene Glycol Monooctyl Ether (C8E4)

Figure 9 shows the surface tension vs the total molality curves at different X_2 values. The m vs X_2 curves were constructed by picking up the m values at a given surface tension from Fig. 9 and are then illustrated by solid lines in Fig. 10. The m value decreases steeply with increasing X_2 in the composition range near $X_2 = 0$ and decreases very slightly in the larger X_2 range. Judging from the existence of a minimum, although it is very shallow, on the m vs X_2 curves at the composition range around $X_2 = 0.9$, we expect a synergistic action between SDS and C8E4 molecules.

The mole fraction of C8E4 in the adsorbed films Y_2 was evaluated by using Eq. (9) and given in the form of m vs Y_2 curves by chained lines together with the m vs X_2 curves

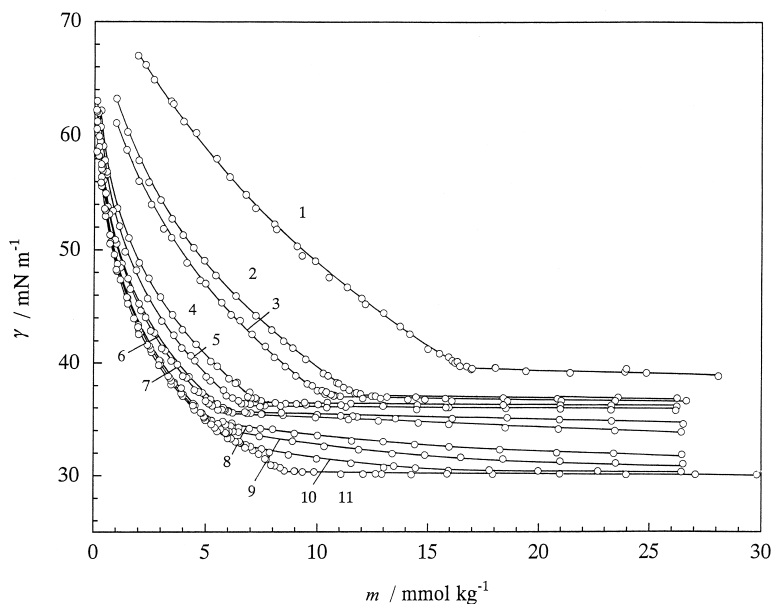


Figure 9 Surface tension vs total molality curves of the SDS-C8E4 system at constant mole fraction: (1) $X_2=0$ (SDS), (2) 0.030, (3) 0.050, (4) 0.200, (5) 0.300, (6) 0.500, (7) 0.600, (8) 0.800, (9) 0.875, (10) 0.9950, (11) 1 (C8E4).

in Fig. 10. Thus Fig. 10 corresponds to the PDA. It should be noted that the m vs Y_2 curves show a negative deviation from the straight line (dotted lines in Fig. 10), showing the ideal mixing in the adsorbed film as given by Eq. (18). Thus an attractive interaction between SDS and C8E4 is undoubtedly demonstrated. Figure 11 shows the PDM of the SDS-C8E4 mixture and reveals the attractive interaction more clearly; the C vs X_2 and then the C vs Z_2 curves have a minimum around $X_2=Z_2=0.8$ and they deviate negatively from the straight line showing an ideal mixing. The PDM in this case shows a negative azeotrope, which is in striking contrast to the positive one demonstrated for the hydrocarbon-fluorocarbon surfactant mixture given in Fig. 7.

The estimated g^{HE} values are obviously negative and their absolute value increases with increasing surface tension as

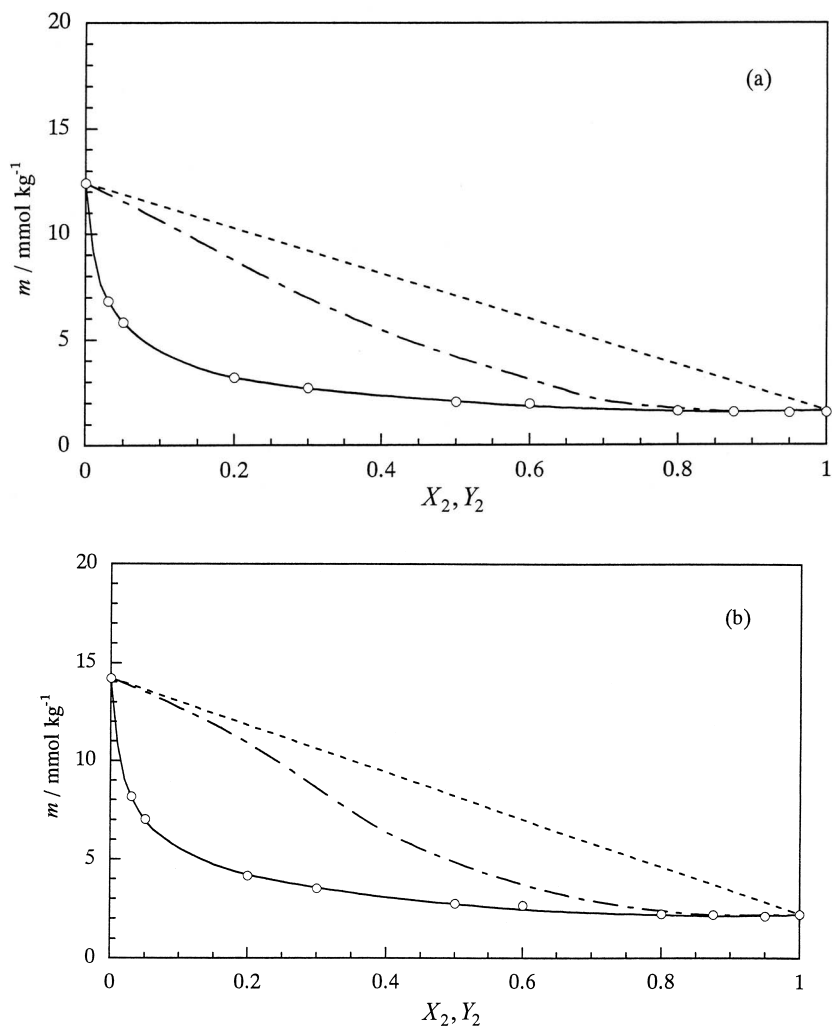


Figure 10 Phase diagram of adsorption of the SDS–C8E4 system: (a) $\gamma = 45 \text{ mN m}^{-1}$, (b) 42.5, (c) 40; (—) m vs X_2 , (---) m vs Y_2 , (.....) ideal mixing.

given in Fig. 12. The former indicates that the interaction between SDS and C8E4 molecules in the adsorbed film is more attractive than that between SDS molecules alone or between C8E4 molecules alone. Taking account of Eq. (44), on the other hand, the latter is related to the packing of the molecules in

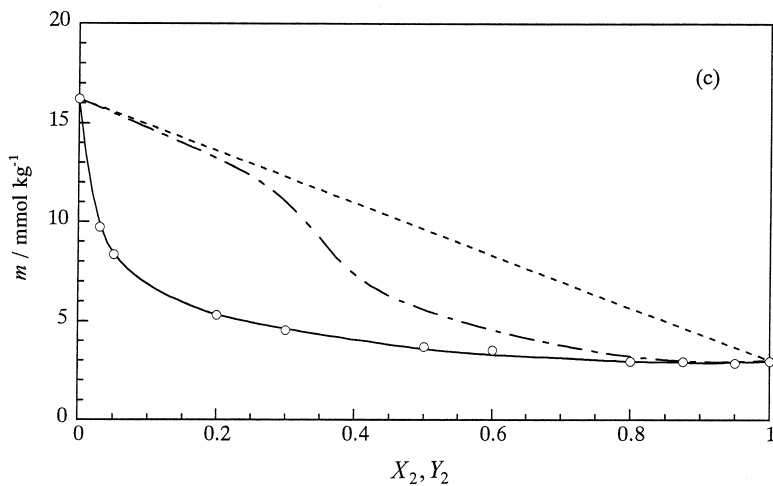


Figure 10 Continued.

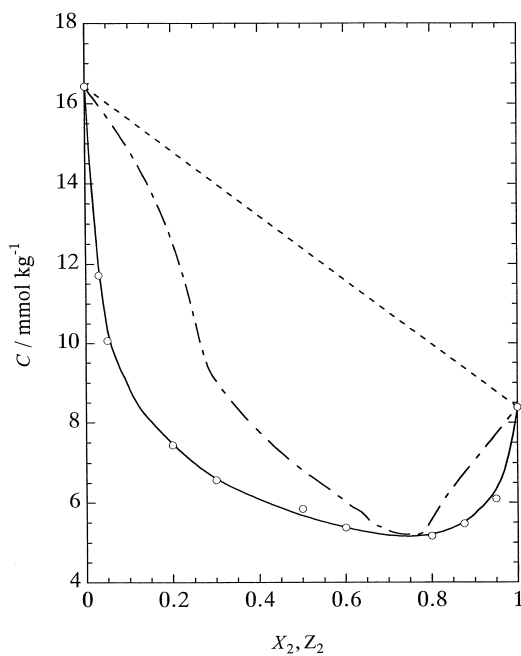


Figure 11 Phase diagram of micelle formation of the SDS-C8E4 system: (—) C vs X_2 , (----) C vs Z_2 , (.....) ideal mixing.

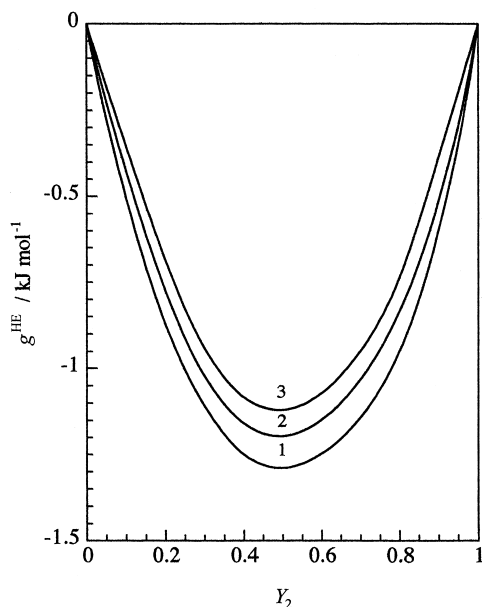


Figure 12 Excess Gibbs free energy of adsorption vs mole fraction in the adsorbed film curves of the SDS-C8E4 system: (1) $\gamma = 45 \text{ mN m}^{-1}$, (2) 42.5, (3) 40.

terms of the excess surface area A^{HE} . It is found that A^{HE} is positive and thus the adsorbed molecules tend to expand its area as compared to the ideal mixing, despite the attractive interaction. If the dispersion forces are mainly responsible for the negative g^{HE} values, the opposite situation must be true; the g^{HE} value changes from the less negative to the more negative one as the distance between hydrophobic chains decreases. We are reasoning from these findings that one of the probable interactions is a kind of anisotropic attraction between the hydrophilic parts of SDS and C8E4 molecules, which has a large optimal interaction distance as compared to the van der Waals interaction. Since this energetically more favorable configuration is expected to be prevented at least partly in the dense assembly of surfactant molecules, the absolute values of g^{HE} in the high surface density region are smaller than those in the low surface density region.

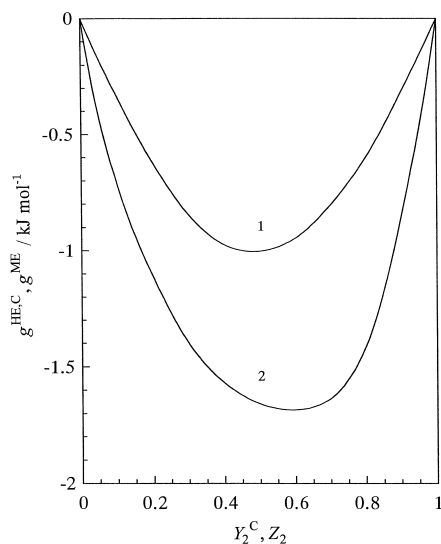


Figure 13 Excess Gibbs free energy of adsorption and micelle formation vs mole fraction curves of the SDS–C8E4 system: (1) $g^{\text{HE,C}}$ vs Y_2^{C} , (2) g^{ME} vs Z_2 .

This is also clearly demonstrated in Fig. 13, where g^{ME} and $g^{\text{HE,C}}$ are plotted against Z_2 and Y_2 at the CMC. The negative g^{ME} value indicates the energetic stabilization accompanied by the micelle formation. Furthermore, the energetic superiority of the mixed micelle formation over the mixed adsorption confirms our idea on the interaction mentioned above: SDS and C8E4 molecules can take a more favorable conformation for the attractive interaction, acting at the long optimal interaction distance in the mixed micelle rather than at that in the mixed adsorbed film because the hydrophilic portion of the molecules and counter ions can effectively use a wedge-like space in a spherical micelle particle in contrast to a cylindrical space in a plane mixed adsorbed film.

2. Dodecylammonium Chloride (DAC)–
Tetraethyleneglycol Monoethyl Ether (C8E4)

The strong attractive interaction between ionic and non-ionic surfactant was observed in the cationic–nonionic

combinations as well as in the anionic-nonionic one of the previous section.

The surface tension of the DAC–C8E4 mixture was measured as a function of the total molality m and the mole fraction of C8E4 X_2 . Since the C vs X_2 curve shows a minimum, some interaction between DAC and C8E4 molecules are certainly expected. The resulting PDM and PDA are given in Figs 14 and 15, respectively. The PDM has an azeotropic point at $X_2 = 0.85$ and shows that a micelle particle abounds in C8E4 compared to the bulk solution at the compositions below the azeotropic point, while in DAC above it. This fact discloses the attractive interaction between DAC and C8E4 molecules in the mixed micelle. The negative deviation of the m vs Y_2 from the straight line given by Eq. (18) also manifests the attractive interaction in the adsorbed film.

Now let us consider the attractive interaction more closely. Our previous studies on the adsorption and micelle formation of cationic surfactant and alcohol mixtures suggested that the deviation from the ideal mixing is caused mainly by

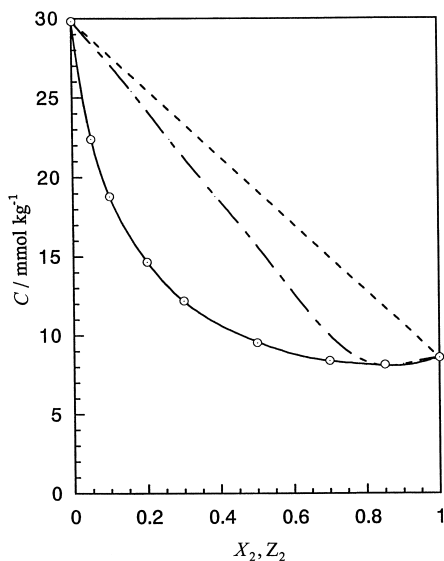


Figure 14 Phase diagram of micelle formation of the DAC–C8E4 system: (—) C vs X_2 , (----) C vs Z_2 , (.....) ideal mixing.

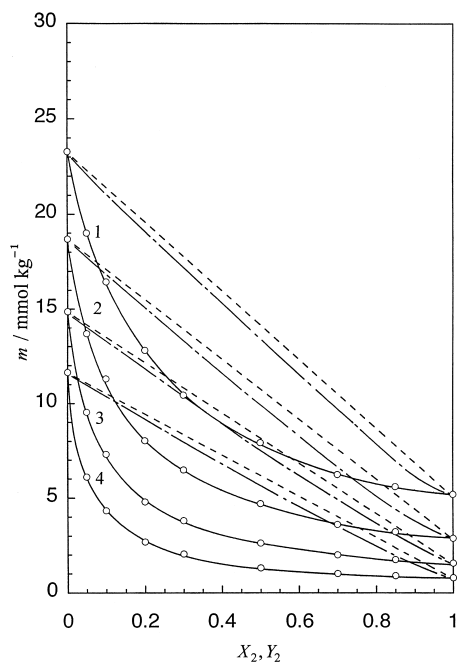


Figure 15 Phase diagram of adsorption of the DAC–C8E4 system: (1) $\gamma = 35 \text{ mN m}^{-1}$, (2) 40, (3) 45, (4) 50; (—) m vs X_2 , (— · — · — ·) m vs Y_2 , (·····) ideal mixing.

two contributions [30], that is, the chemical nature of the components and the packing of the surfactant molecules in the aggregates. Considering the chemical nature that DAC dissociates into surfactant ions and counter ions and C8E4 has a nonionic polar head group, there probably exists some kind of electrostatic interaction such as an ion-dipole one. With respect to the packing molecule, on the other hand, the positive excess surface area evaluated by using Eq. (44) suggests that the mixing of DAC and C8E4 molecules in the adsorbed film causes an increase in the area. This may imply that the interaction is not favorable from the standpoint of the occupied area. Therefore, it is said that the attractive interaction of this system comes from the electrostatic interaction.

The influence of the geometry on the interaction is clearly demonstrated by comparing the excess Gibbs free energy of

micelle formation g^{ME} to that of adsorption at the CMC $g^{\text{HE,C}}$ in Fig. 16. The g^{ME} value is much more negative than that in the adsorbed film, which suggests that C8E4 molecules have a long and bulky hydrophilic part and DAC molecules probably can take a more favorable conformation for the attractive interaction in the mixed micelle than in the adsorbed film because molecules can share a wedge-like space in a spherical micelle particle as already described in the previous section.

Taking note that the attractive interactions between the ionic surfactant and the nonionic one is observed irrespective of the ionic nature of the ionic surfactants, let us propose the scheme of the attractive interaction. In our previous paper on the adsorption and micelle formation of the aqueous solutions of HCl–C8E4 and NaCl–C8E4 mixtures [27], we have examined the interaction between H^+ , Na^+ , and Cl^- ions with C8E4

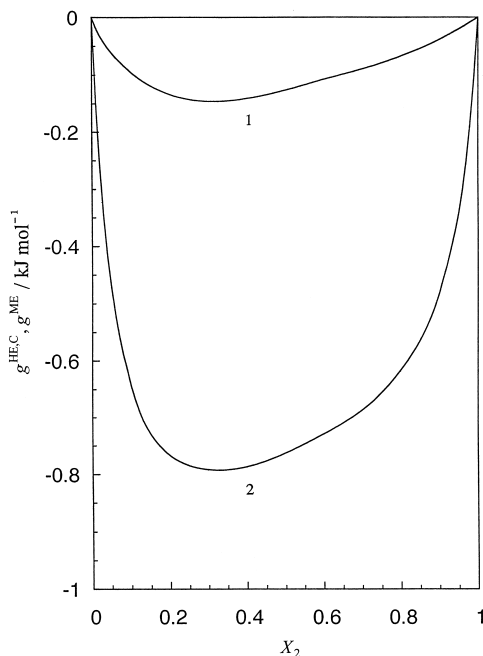


Figure 16 Excess Gibbs free energy of adsorption and micelle formation vs mole fraction curves of the DAC–C8E4 system: (1) $g^{\text{HE,C}}$ vs X_2 , (2) g^{ME} vs X_2 .

molecules and demonstrated that ether oxygen interacts attractively with cationic species both in the adsorbed films and in the micelles from the PDA and PDM [27]. On the basis of this view, we have concluded that the attractive interaction in the DAC–C8E4 mixtures originates from the ion–dipole interaction or hydrogen bonding between the ammonium group and oxygen atom of the ethylene oxide group because the counter ion does not play an important role for the attractive interaction.

With respect to the attractive interaction in the SDS–C8E4 system, on the other hand, an indirect interaction between DS^- and the ether oxygen through Na^+ ions seems to be plausible because of the following findings:

1. The ether oxygens of C8E4 do not interact attractively with anionic species, but with the cationic species mentioned above.
2. The excess Gibbs energies of the SDS–C8E4 system are more negative than those of the DAC–C8E4 system as demonstrated in Fig. 17. Nevertheless, DA^+ ions are likely to interact rather directly with the hydrophilic part of C8E4 as mentioned in (1).
3. The positive excess area suggests that, when DS^- ions and C8E4 molecules interact in the adsorbed film, they are at a longer distance compared to an ideal distance despite a strong attractive interaction between them.

Summarizing the interaction scheme, the Na^+ counter ions contribute to the stabilization in the SDS–C8E4 system, whereas the DS^- ions interact indirectly with C8E4 through Na^+ ions. On the other hand, the DA^+ ions interact directly with C8E4 in the DAC–C8E4 system.

C. Ionic–Ionic Surfactant Mixtures

1. Decylammonium Chloride
(DeAC)–Dodecylammonium Chloride (DAC)

The mole fractions Y_2 and Z_2 were evaluated by applying Eqs (32) and (35) to the surface tension data [31]. The PDA at 40 mN m^{-1} and PDM are given in Fig. 18 [11]. Judging from

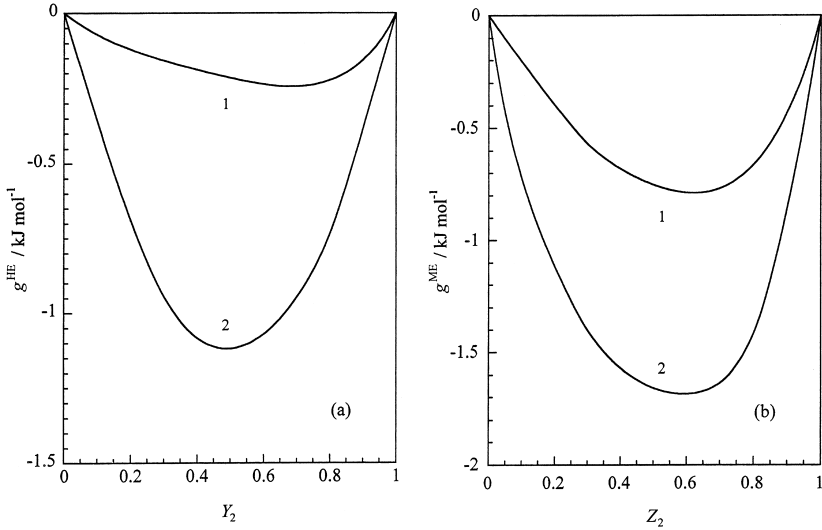


Figure 17 (a) Excess Gibbs free energy of adsorption at 40 mN m^{-1} vs mole fraction in the adsorbed film curves: (1) DAC-C8E4 system, (2) SDS-C8E4 system. (b) Excess Gibbs free energy of micelle formation vs mole fraction in the micelle curves: (1) DAC-C8E4 system, (2) SDS-C8E4 system.

that the surfactants are analogues with each other having the difference of the carbon number only by two and the same counter ion and also the shape of the diagram is similar to that of a cigar, one may expect the ideal mixing of DeAC and DAC molecules in the adsorbed film and micelle.

However, comparing the m vs Y_2 curves with the ones showing the ideal mixing of Eq. (34) with $\nu = 2$ given by

$$m^2 = (m_1^0)^2 + [(m_2^0)^2 - (m_1^0)^2]Y_2 \quad (45)$$

we note that the adsorbed film is enriched slightly in the more surface active DAC molecules than in the less surface active DeAC molecules compared to the adsorbed film of the ideal mixing. Taking note of the equation of the ideal mixing in micelle given by

$$C^2 = (C_1^0)^2 + [(C_2^0)^2 - (C_1^0)^2]Z_2 \quad (46)$$

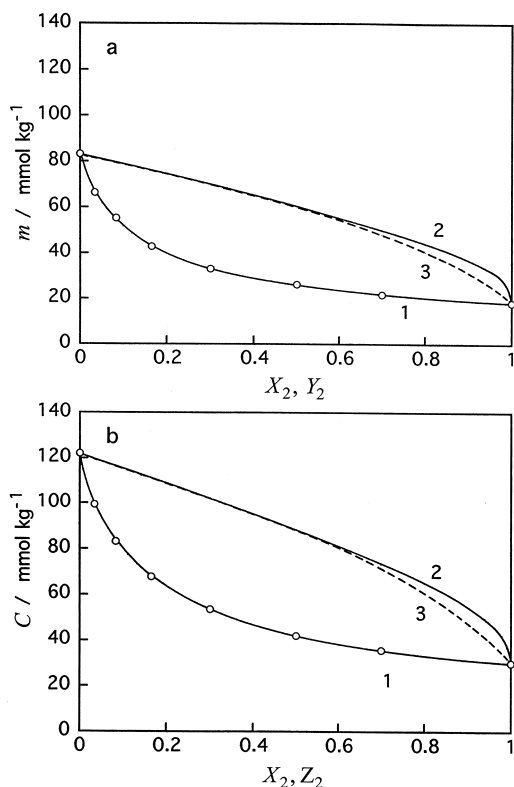


Figure 18 (a) Phase diagram of adsorption of the DeAC–DAC system at 40 mN m^{-1} : (1) m vs X_2 , (2) m vs Y_2 , (3) ideal mixing. (b) Phase diagram of micelle formation of the DeAC–DAC system: (1) C vs X_2 , (2) C vs Z_2 , (3) ideal mixing.

it is noted that the situation in the micelle is very similar to that in the adsorbed film. This example shows that, even in the mixture of analogues, nonideal mixing happens and is revealed only based on the correct criterion of ideal mixing given by Eqs (45) and (46).

2. Decylammonium Bromide (DeAB)–Dodecylammonium Chloride (DAC)

The only difference of this mixture from the DeAC–DAC is that the counter ion is not common in the DeAB–DAC but common

in the DeAC–DAC system. However, we realize that this difference leads to a large nonideal mixing as follows [11].

The mole fractions Y_2 and Z_2 were evaluated by applying Eqs (9) and (22) to the surface tension data [32]. The PDA at 40 mN m^{-1} and PDM are given in Fig. 19 [11]. First it is seen that the m vs Y_2 and C vs Z_2 curves are convex downward and then the nonideal mixing in both the adsorbed film and micelle is expected. Here it should be noted that the ideal mixing is given by the straight lines of Eqs (18) and (25), in contrast to the quadratic equations given by Eqs (45) and (46). The excess Gibbs free energies were calculated from the respective PDAs and PDM and shown in Fig. 20 together with the corresponding

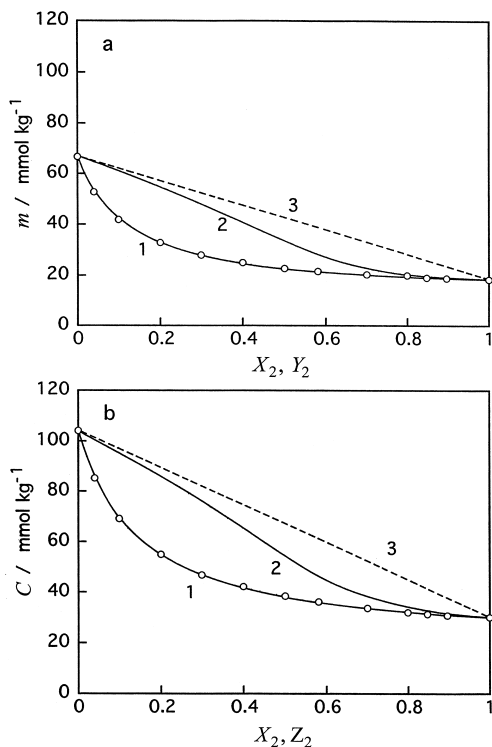


Figure 19 (a) Phase diagram of adsorption of the DeAB–DAC system at 40 mN m^{-1} : (1) m vs X_2 , (2) m vs Y_2 , (3) ideal mixing; (b) Phase diagram of micelle formation of the DeAB–DAC system: (1) C vs X_2 , (2) C vs Z_2 , (3) ideal mixing.

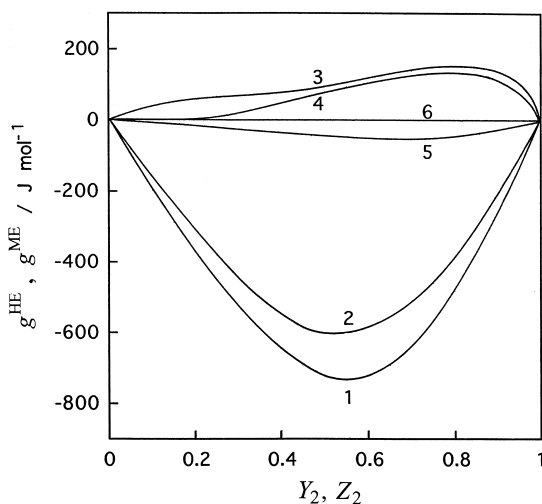


Figure 20 Excess Gibbs free energy of adsorption at 40 mN m^{-1} and micelle formation vs mole fraction curves: (1) g^{HE} vs Y_2 of the DeAB–DAC system, (2) g^{ME} vs Z_2 of the DeAB–DAC system, (3) g^{HE} vs Y_2 of the DeAC–DAC system, (4) g^{ME} vs Z_2 of the DeAC–DAC system, (5) g^{HE} vs Y_2 of the DeAC–DeAB system, (6) g^{ME} vs Z_2 of the DeAC–DeAB system.

values of the DeAC–decylammonium bromide (DeAB) system [33]. Judging from the results of the DeAC–DeAB system where the surfactant cations are common to each other, chloride and bromide ions mix ideally in the micelles and very slightly nonideally in the adsorbed films. Since the activity coefficients arising from preferential adsorption is less than unity whenever the preferential adsorption takes place [11], the negative g^{HE} comes from the preferential adsorption of bromide ions to chloride ions and this coincides with the observation that the mole fraction Y_2 is shifted to the DeAB side from the ideal mixing line. This preferential adsorption is more pronounced in the DeAB–DAC mixtures, of which g^{HE} is largely negative compared to that of the DeAC–DeAB system. Taking account of the finding that the adsorbed film of the DeAC–DAC mixture abounds more in DA^+ than DeA^+ compared to the ideal mixing, the results of the DeAB–DAC system clearly indicates that attractive interaction, and thus negative values of g^{HE} due to

the preferential adsorption of bromide ions to chloride ions, overcomes the small positive values of g^{HE} due to nonideal mixing of hydrophobic chains.

Thus the examination in terms of the excess Gibbs energy reveals the miscibility of surfactant molecules from the viewpoint of not only the surfactant ions but also counter ions such as the preferential adsorption.

IV. TRANSITION BETWEEN TWO STATES OF BINARY SURFACTANT MIXTURES

Mixing of surfactants often produces synergetic action, new functions, and new organized molecular assemblies. In this section, first the spontaneous vesicle formation followed by micelle formation is demonstrated with respect to a cationic–anionic surfactant mixture. The vesicles of cationic–anionic surfactant mixtures are often called catanionic vesicles, which were reviewed thoroughly and very recently by Tondre and Caillet [34]. Here the spontaneous formation of catanionic vesicles were studied by measuring surface tension and by constructing the phase diagram of vesicle and micelle formation by applying the thermodynamic method [8]. Second, the adsorption of long chain hydrocarbon and fluorocarbon alcohol mixtures from their oil solution to the oil/water interface will be demonstrated and their miscibility in the adsorbed film will be proved to be greatly changed by the phase transition of the adsorbed film [9,10].

Thus, the transition in the aqueous solution between micelle and vesicle for the binary water–soluble surfactant mixture and that in the adsorbed film between the expanded and condensed states for the binary oil–soluble surfactant mixture will be shown.

A. Vesicle–Micelle Transition of Sodium Decyl Sulfate (SDeS)–Decyltrimethylammonium Bromide (DeTAB) Mixture

The surface tension of the mixture was carefully measured as a function of the total molality defined by Eq. (3) with $\nu_1 = \nu_2 = 1$

at the fixed mole fraction of DeTAB [8]. The molality at the critical micelle concentration CMC, C^M , and that at the critical vesicle concentration CVC, C^V , were determined from the γ vs m curves. Then the phase diagram of aggregate formation was constructed by using the thermodynamic consideration. First the simple model of the total molality vs mole fraction diagram of aggregate formation will be described and then the experimental results followed by thermodynamic analysis will be demonstrated.

1. Simple Model of the Molality vs Mole Fraction Diagram of Aggregate Formation

Micelles and vesicles are not macroscopic phases in the thermodynamic sense because they never exist separately from the solution. However, when their thermodynamic quantities are defined in terms of the excess ones, the thermodynamic theory of micelle formation, in which micelle particles are treated as if they are macroscopic ones, has been successful in understanding micelle formation and properties in the solution [7,14]. Then we show a very simple way to predict the coexisting regions of vesicles and micelles in the total molality vs mole fraction of the surfactant diagram by using our thermodynamic method and the mass balance equation.

In the SDeS–DeTAB system, each pure surfactant does not form vesicles but the mixture does in a limited mole fraction range because the strong electrostatic molecular interaction between the two surfactant ions results in a kind of synergism. Thus the concentration of aggregate formation C is decreased steeply from their respective pure CMC values by adding the other component. An example of such C vs X_2 behavior is illustrated by the three curves connected at two break points at C^t and X_2^t s where the vesicle–micelle transition is assumed to take place as shown in Fig. 21, where C_1^0 and C_2^0 are the CMCs of the respective pure surfactants.

The mole fraction of the second component in the micelle Z_2^M is evaluated by applying [see Eq. (22)]

$$Z_2^M = X_2 - (X_1 X_2 / C^M) (\partial C^M / \partial X_2)_{T,p} \quad (47)$$

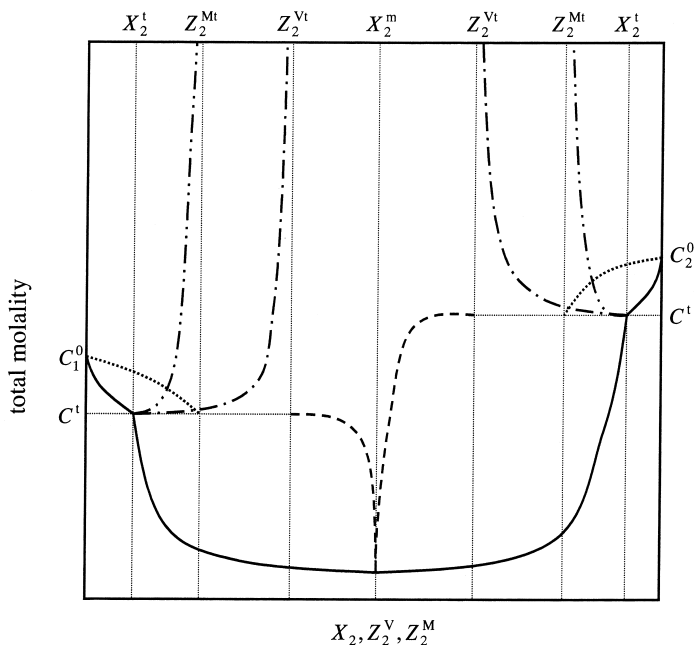


Figure 21 Total molality vs mole fraction diagram predicted: (—) C^M vs X_2 at $0 \leq X_2 \leq X_2^t$ and $X_2^t \leq X_2 \leq 1$, C^V vs X_2 at $X_2^t \leq X_2 \leq X_2^m$ and $X_2^m \leq X_2 \leq X_2^t$, (.....) C^M vs Z_2^M at $0 \leq Z_2^M \leq Z_2^{Mt}$ and $Z_2^{Mt} \leq Z_2^M \leq 1$, (----) C^V vs Z_2^V at $Z_2^{Vt} \leq Z_2^V \leq Z_2^m$ and $Z_2^m \leq Z_2^V \leq Z_2^{Vt}$, (-.-.-) m^I vs X_2 , (-.-.-) m^{II} vs X_2 .

to the critical micelle concentration C^M vs X_2 curves and similarly the mole fraction of the second component in the vesicle Z_2^V is evaluated by applying

$$Z_2^V = X_2 - (X_1 X_2 / C^V) (\partial C^V / \partial X_2)_{T,p} \quad (48)$$

to the critical vesicle concentration C^V vs X_2 curves. The C^M vs Z_2^M and C^V vs Z_2^V are schematically shown in Fig. 21, where Z_2^{Mt} and Z_2^{Vt} are the mole fractions in the micelle and vesicle at the vesicle-micelle transition point.

When vesicles and micelles are in equilibrium with each other in the solution, the mass balance relations for the total surfactants and surfactant 2 are respectively given by

$$m = C^t + m^M + m^V \quad (49)$$

and

$$mX_2 = C^t X_2^t + m^M Z_2^{Mt} + m^V Z_2^{Vt} \quad (50)$$

Here we assumed that the monomer concentration is equal to C^t and the mole fractions in vesicle and micelle are equal to Z_2^{Vt} and Z_2^{Mt} , respectively, and they do not change as the total concentration is further increased because vesicle and micelle are assumed to be a kind of macroscopic phase. Let us examine the right-hand part of the diagram of Fig. 21. At the composition region $Z_2^{Vt} < X_2 < Z_2^{Mt} < X_2^t$, the total molality m^I at which micelle formation starts to take place in the vesicle solution is obtained by putting $m^M = 0$ as

$$m^I = C^t(X_2^t - Z_2^{Vt})/(X_2 - Z_2^{Vt}) \quad (51)$$

At the composition region $Z_2^{Vt} < Z_2^{Mt} < X_2 < X_2^t$, on the other hand, the total molality m^{II} at which vesicle disappears is obtained by putting $m^V = 0$ as

$$m^{II} = C^t(X_2^t - Z_2^{Mt})/(X_2 - Z_2^{Mt}) \quad (52)$$

Therefore the m^I vs X_2 and m^{II} vs X_2 curves are predictable once the values of X_2^t , Z_2^{Mt} , and Z_2^{Vt} are experimentally obtained. Taking account of the relation

$$\begin{aligned} m^I - C^V &= C^t(X_2^t - Z_2^{Vt})/(X_2 - Z_2^{Vt}) - C^V \\ &> C^V(X_2^t - X_2)/(X_2 - Z_2^{Vt}) > 0 \end{aligned} \quad (53)$$

we note that vesicle formation takes place in preference to micelle formation in the vesicle–micelle coexistence regions.

By using the diagram given in Fig. 21, the change of γ with m at a given X_2 can be predicted qualitatively as is schematically illustrated in Fig. 22 with respect to the right-hand side of Fig. 21 ($X_2^m < X_2$), where X_2^m is the mole fraction at the minimum of the C vs X_2 curve. Curve 1 (pure second surfactant $X_2=1$) has one break point at the CMC and the surface tension is practically constant above the CMC.

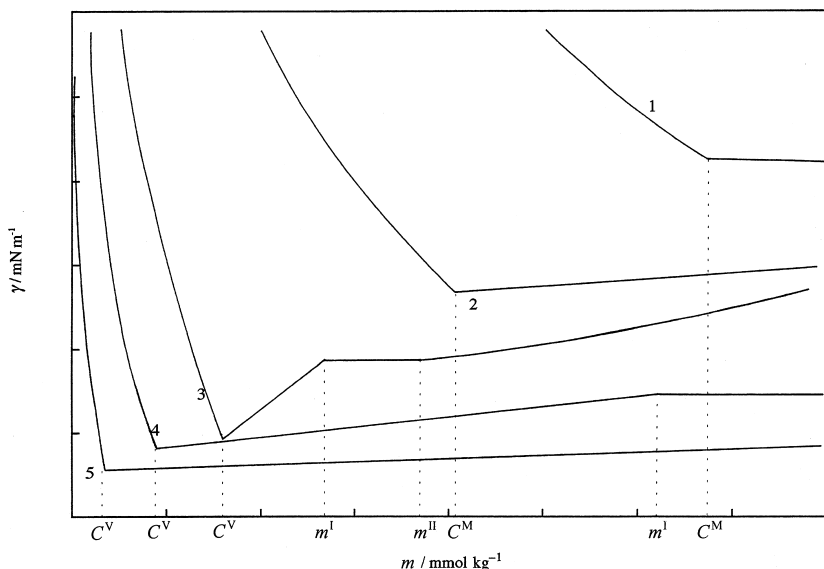


Figure 22 Surface tension vs total molality curves predicted: (1) $X_2=1$, (2) $X_2^t < X_2 < 1$, (3) $Z_2^{Mt} < X_2 < X_2^t$, (4) $Z_2^{Vt} < X_2 < Z_2^{Mt}$, (5) $X_2^m < X_2 < Z_2^{Vt}$.

Curve 2 ($X_2^t < X_2 < 1$) has one break at the CMC and the surface tension increases with the molality due to the change of the micelle and monomer compositions. Curve 3 ($Z_2^{Mt} < X_2 < X_2^t$) has three break points at C^V , m^I , and m^{II} . It is expected that the surface tension at the concentrations between m^I and m^{II} is constant due to the vesicle–micelle coexistence. The changes of the surface tension before and after the constant surface tension show the changes of vesicle and micelle compositions with m . On Curve 4 ($Z_2^{Vt} < X_2 < Z_2^{Mt}$), vesicles and micelles start to coexist at m^t and vesicles never vanish even at high m^I and therefore the surface tension is constant at concentration above m^I . Finally Curve 5 ($X_2^m < X_2 < Z_2^{Vt}$) has only one break corresponding to the CVC. The shape of the curves at $X_2^m < X_2$ is qualitatively similar to that at $X_2 < X_2^m$. The qualitative behavior predicted by this simple model will be compared to the one obtained from the thermodynamic analysis of the experimental results.

2. Vesicle Formation and Vesicle–Micelle Transition

Figure 23 shows the surface tension vs total molality curves at the mole fractions of the DeTAB-rich region [8]. We see that the variation of γ with m at low molalities and at X_2 below 0.98 looks like that of a usual surfactant mixture: the surface tension decreases very rapidly as the total molality increases and is almost constant above a break point. However, the dynamic light scattering measurement suggested the existence of much larger aggregates than micelle particles with the average radius of approximately 500 nm. The vesicle particles were observed by using the optical microscope at some X_2 and also in the TEM image of freeze-fracture replicas. Thus it is concluded that the first break points on these γ vs m curves are referred to as the critical vesicle concentration C^V .

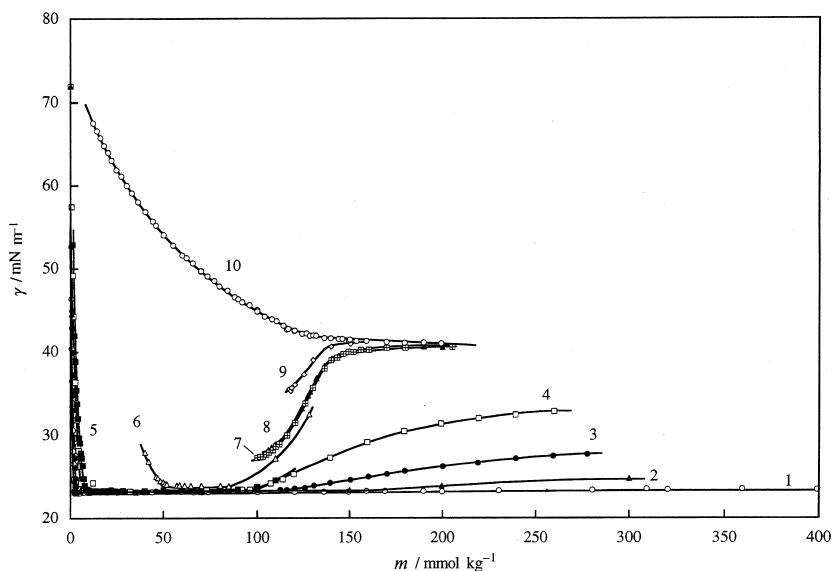


Figure 23 Surface tension vs total molality curves of the SDeS–DeTAB system at constant mole fraction: (1) $X_2 = 0.7012$, (2) 0.8004, (3) 0.9000, (4) 0.9700, (5) 0.9800, (6) 0.9990, (7) 0.9996, (8) 0.9997, (9) 0.9999, (10) 1.

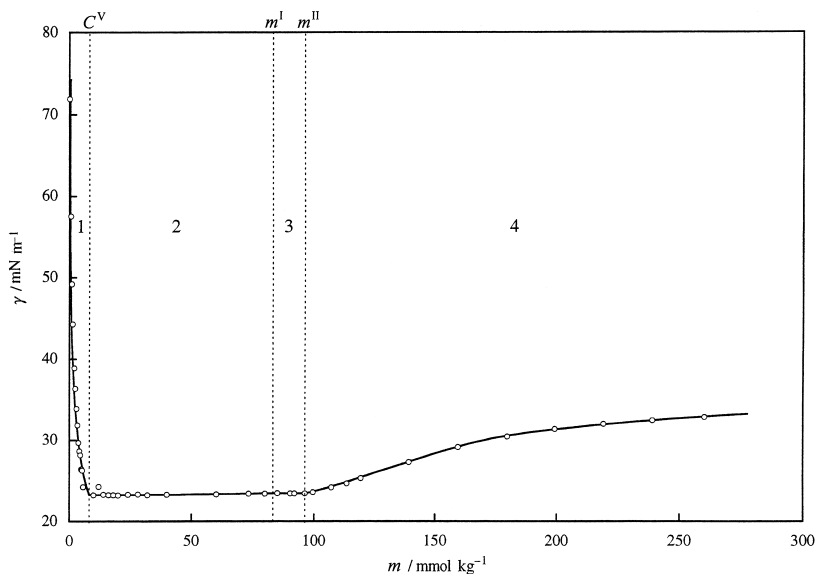


Figure 24 Surface tension vs total molality curves of the SDeS-DeTAB system at $X_2=0.9700$: (1) monomer, (2) monomer + vesicle, (3) monomer + vesicle + micelle, (4) monomer + micelle.

Examining more closely the curves and taking account of the visual and optical observations, we have concluded that four regions exist on each curve: the example at $X_2=0.9700$ is illustrated in Fig. 24. Region 1 corresponds to the monomer solution and the surface tension decreases steeply within a very narrow concentration range. In Region 2, the surface tension increases slightly but definitely with m . The solutions were turbid and slightly bluish, although the bluish color disappeared completely by freezing them followed by thawing and birefringent at some total molalities. It was expected from the turbidity that the aggregates have a size of micrometer order and in fact a donut-like shape with a size of a few micrometers was observed by differential interference microscope. Furthermore the aggregates formed in the birefringent solution may have lamellar structures because a sheet-like structure was vaguely observed with the differential interference microscope. It should be noted that the surface tension falls on the same curve despite the changes in the structures. In Region 3,

the surface tension is constant and solution is observed to be bluish and transparent. It should be pointed out that the appearance of the solution and the γ values were not changed by freezing the solution followed by thawing it and the solution appeared to be bluish and transparent even at the highest total molality of this region. Judging from the appearance of the solution and the fact that vesicles were hardly observed by optical microscopy, the size of vesicles in this region is probably around 100 nm or less. In Region 4, it is important to note a new observation, which is not found in the ordinary mixed micelle systems, that the γ value starts to increase again with m . The solutions become completely clear and colorless. This suggests the absence of vesicle particles. The curves No. 1 to No. 5 in Fig. 23 are similar in their shapes.

Comparing the γ vs m curves obtained from the experiments to that from the simple theory given in Fig. 22, we note the fairly good correspondence between them. Thus, in Region 1, the surfactant monomers are dispersed in the solution and vesicles of the surfactant mixture spontaneously form at C^V . In Region 2, the vesicles and monomers are dispersed in the solution. The composition of the vesicle is different from that in monomeric states. In Region 3, micelles of the surfactant mixture appear at m^I and then the vesicles, micelles, and monomers are dispersed in the solution. Judging from the experimental finding that the surface tension is constant in this region, it is probable that the aqueous solution system behaves as if it has three kinds of macroscopic phases, that is, monomer solution, micelles, and vesicles. The molality is further increased up to m^{II} , vesicle particles disappear and then micelle particles and monomer are dispersed in the solution in Region 4.

Let us evaluate the mole fraction of DeTAB Z_2^V by applying Eq. (48) to the C^V vs X_2 curve given by the open circles on the solid line. The results are drawn by chained line in Fig. 25. The C^V vs X_2 and the C^V vs Z_2^V diagram is called the phase diagram of vesicle formation. It is very important to note that the Z_2^V values are close to 0.5 at most of bulk compositions: a vesicle particle contains almost equal numbers of surfactant cations and anions irrespective of the bulk compositions even when the monomer solution being in equilibrium with the vesicle

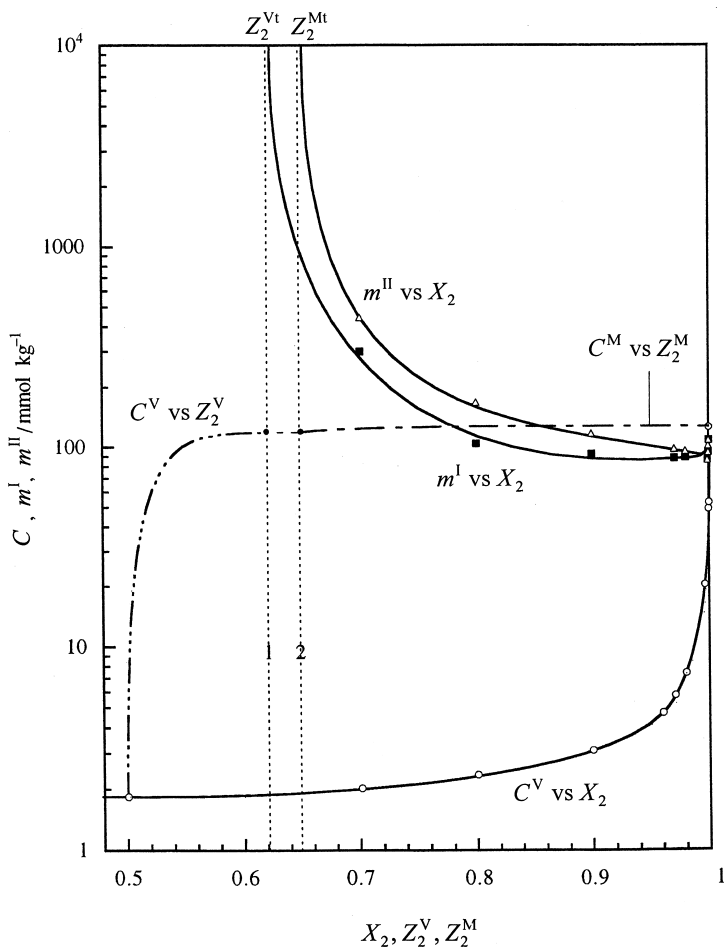


Figure 25 Total molality vs mole fraction diagram of the SDeS-DeTAB system: (1) asymptote of the m^I vs X_2 curve, (2) asymptote of the m^{II} vs X_2 curve.

particles are only 0.01 mol% surfactant anions. The m^I and m^{II} values from the experiments are plotted against X_2 . Here the expected C^M vs Z_2^M curve is also shown, which was not obtained because of its experimental difficulty but is anticipated from the present results. The broken lines are the asymptotes of the m^I and m^{II} vs X_2 curves suggested by the simple theory

mentioned above. We note the good correspondence of the experimental results given in Fig. 25 to the prediction from the simple theory illustrated in Fig. 21.

Thus spontaneous vesicle formation and vesicle–micelle transition are well described by our thermodynamic method developed for mixed micelle formation: the concentration vs composition diagram can predict the critical vesicle and micelle concentrations, the concentration region of the vesicle–micelle coexistence. Furthermore, the change of surface tension with total molality with the composition X_2 can be predicted by using the concentration vs composition diagram.

B. Phase Transition and Miscibility in the Adsorbed Films of 1-Icosanol (C₂₀OH) and 1,1,2,2-Tetrahydroheptadecafluorodecanol (FC₁₀OH)

As shown in Section III.A.2, the mutual interaction between hydrocarbon and fluorocarbon chains is very weak so that some mixtures of hydrocarbon and fluorocarbon surfactants are de-mixed or have a tendency of de-mixing in their micelle. At the aqueous solution/air (or oil) interfaces, however, even these water-soluble surfactants are miscible with each other at all proportions. This is at least partly because the water soluble surfactants have ionic or large size of hydrophilic groups and then close packing of hydrophobic chains at the interface is hardly realized due to the electrostatic or steric repulsion of the hydrophilic groups compared to that in the micelle, where a rather large distance between hydrophilic head groups is available. Therefore it is of great interest to investigate the adsorption of the oil-soluble mixtures of nonionic hydrocarbon and fluorocarbon compounds at the water/oil solution of the mixture. From this viewpoint, the adsorption of long chain hydrocarbon and fluorocarbon alcohols, and also their mixtures at oil/water interfaces have been studied systematically: the phase transition in the adsorbed film often is observed and influenced greatly by temperature, pressure, and also mixing with other compounds [35]. The phase transition observed in our studies has been proved and studied much more from the

viewpoint of the molecular structure at the interface by synchrotron X-ray reflection and scattering techniques [36].

1. The Phase Transition in the Adsorbed Film of the Mixture

The interfacial tension γ of the hexane solution of FC10OH and C20OH mixture/water system was measured as a function of the total molality m and the mole fraction of FC10OH X_2 at 298.15 K under atmospheric pressure [9]. The results at the mole fractions below 0.275 and above 0.280 are shown together with those of the respective pure alcohols in Figs 26(a) and (b), respectively. It is realized that all the curves have a distinct break point at which the slope of the curve increases greatly. Furthermore it should be noted that the two break points were observed on the curves at $X_2 = 0.275$ and 0.280 as indicated by the arrows. The break points on the γ vs m curves suggest that one or two kinds of phase transition occur in the adsorbed film of the mixture. In the following, we call the break points at the higher molality at $X_2 = 0.275$ and 0.280 the second break point and the others the first one.

In Fig. 27, the interfacial tension γ^{eq} and the total molality m^{eq} at the break points are plotted against X_2 . It is seen that the γ^{eq} vs X_2 curve of the first break point has a sharp-pointed minimum and the corresponding m^{eq} vs X_2 curve has a sharp-pointed maximum. The corresponding curves of the second break touch the curves of the first break at their extremum. Thus the three different states shown by A, B, and C are suggested in the adsorbed films of the FC10OH and C20OH mixture.

To identify these three states in the adsorbed films, the interfacial pressure π and the mean area per adsorbed molecule A were calculated according to the usual way and demonstrated as the π vs A curves in Fig. 28. Figure 28(a) and (b) show that the curves consist of two parts connected by one discontinuous change in A : the gradual increase and the steep one in π with decreasing A . It is noted that the A values converge at about 0.2 nm^2 below $X_2 = 0.250$ and at about 0.3 nm^2 above $X_2 = 0.300$, respectively. Judging that the cross-sectional area

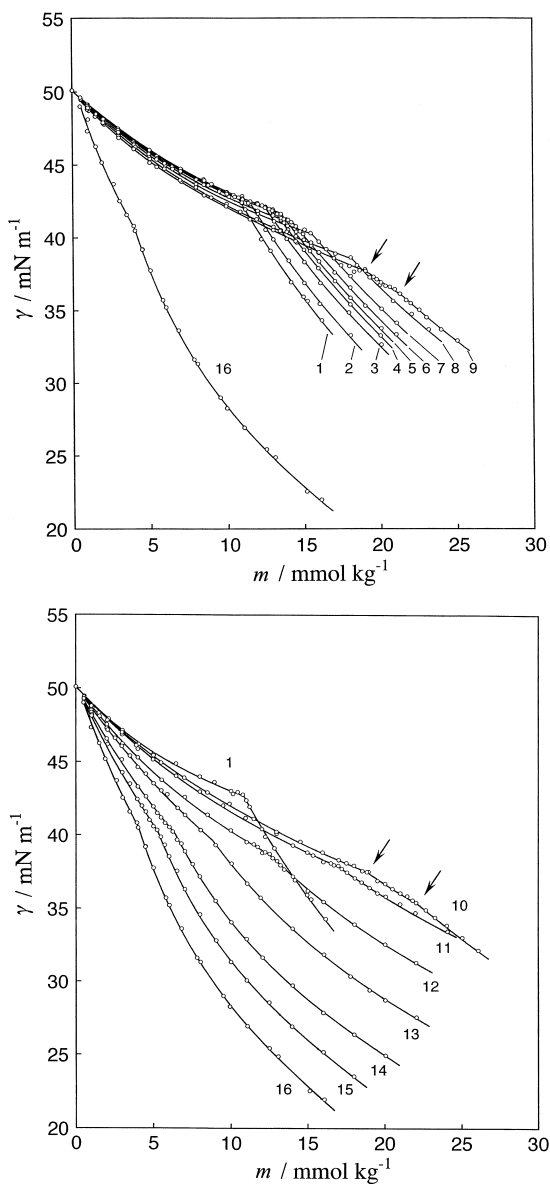


Figure 26 Interfacial tension vs total molality curves of the C20OH-FC10OH system at constant mole fraction: (1) $X_2=0$, (2) 0.050, (3) 0.100, (4) 0.125, (5) 0.150, (6) 0.170, (7) 0.200, (8) 0.250, (9) 0.275, (10) 0.280, (11) 0.300, (12) 0.375, (13) 0.500, (14) 0.650, (15) 0.800, (16) 1.

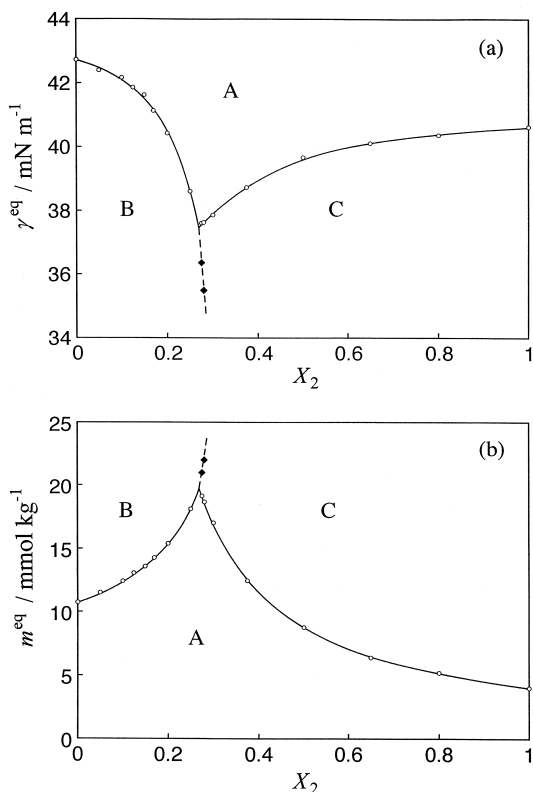


Figure 27 (a) Equilibrium interfacial tension vs mole fraction curves of the C20OH-FC10OH system: (\odot) first break point, (\bullet) second break point; (b) Equilibrium total molality vs mole fraction curves of the C20OH-FC10OH system: (\odot) first break point, (\bullet) second break point.

of hydrocarbon and fluorocarbon chains are very close to these A values, we have concluded that the phase transition takes place from the expanded to the condensed state at the first break points. Furthermore the convergence of A at the two different values suggests that the condensed film is constructed of C20OH molecules solely at $X_2 \leq 0.250$ and FC10OH solely at $X_2 \geq 0.300$, respectively. On the other hand, judging the finding that the A value of the expanded state varies continuously with the mole fraction X_2 , the film is probably constructed by these

alcohol mixtures. The composition relation between the bulk solution and the adsorbed film will be clarified by drawing the phase diagram of adsorption as demonstrated below.

Now let us look closely at the second break points at $X_2 = 0.275$ and 0.280 . The π vs A curves are given together with those of the pure alcohols in Fig. 28(c). Examining these curves, we can say that the first break points correspond to the phase transition from the expanded state to the condensed film of FC10OH and the second to that from the condensed film of FC10OH to the condensed film of C20OH, respectively. Thus it is concluded that the three regions A, B, and C correspond to the expanded, C20OH condensed, and FC10OH condensed state, respectively. When the different species of these alcohol molecules are completely immiscible with each other in the C20OH and FC10OH condensed states, the thermodynamic relation can predict that the phase transition should take place from the condensed film of FC10OH to that of C20OH and that its reverse does not take place [9].

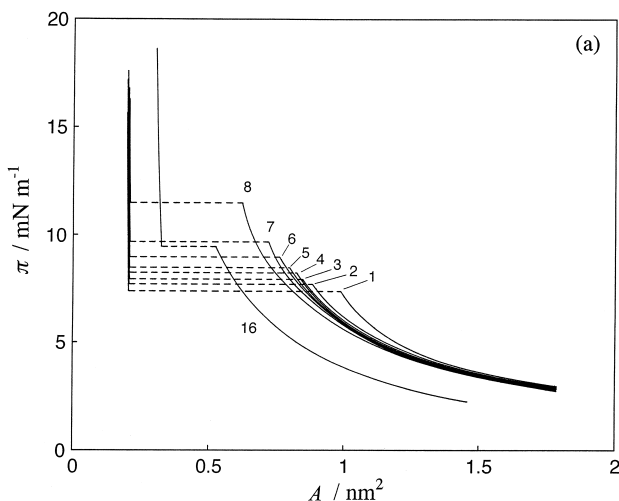


Figure 28 Interfacial pressure vs area per adsorbed molecule curves of the C20OH-FC10OH system at constant mole fraction: (1) $X_2 = 0$, (2) 0.050, (3) 0.100, (4) 0.125, (5) 0.150, (6) 0.170, (7) 0.200, (8) 0.250, (9) 0.275, (10) 0.280, (11) 0.300, (12) 0.375, (13) 0.500, (14) 0.650, (15) 0.800, (16) 1.

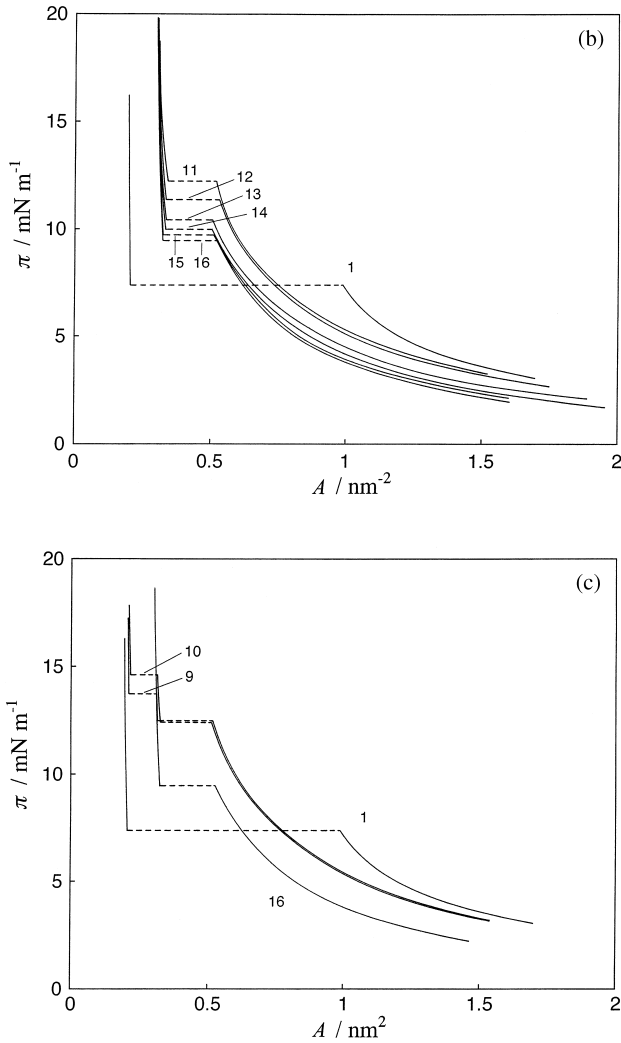


Figure 28 Continued.

2. Miscibility in the Adsorbed Film of the Mixture

To make sure the conclusion on the miscibility in the adsorbed film derived from the π vs A curves and to get more quantitative information on the miscibility, let us construct the phase diagram of adsorption PDA at different interfacial

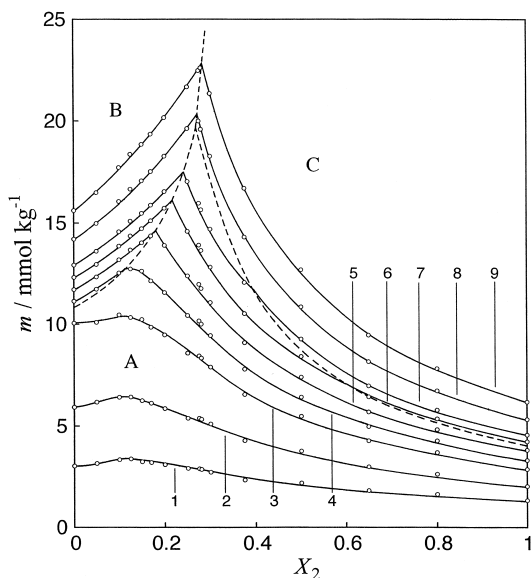


Figure 29 Total molality vs mole fraction curves of the C20OH-FC10OH system at constant interfacial tension: (1) $\gamma = 47 \text{ mN m}^{-1}$, (2) 45, (3) 43, (4) 42, (5) 41, (6) 40, (7) 39, (8) 37, (9) 35; (----) m^{eq} vs X_2 .

tension values [10]. The mole fraction of FC10OH in the adsorbed film Y_2 was evaluated by applying Eq. (9) to the total molality m vs the mole fraction in the hexane solution X_2 curves given in Fig. 29, where the broken lines show the phase transition points as already given in Fig. 27(a). The PDAs are demonstrated at some selected γ values in Fig. 30.

Figure 30(a) shows the PDA at 45 mN m^{-1} where the adsorbed films are all in the expanded states. It is seen that C20OH and FC10OH molecules are miscible at all the proportions and their mixture forms a positive azeotrope at about $X_2 = 0.1$: the adsorbed film is richer in C20OH molecules below and in FC10OH molecules above the azeotropic point than the bulk oil solutions. Since the m vs Y_2 curve deviates positively from the straight line of the ideal mixing given by Eq. (18), the molecular interaction between different species is less attractive compared to that between the same species.

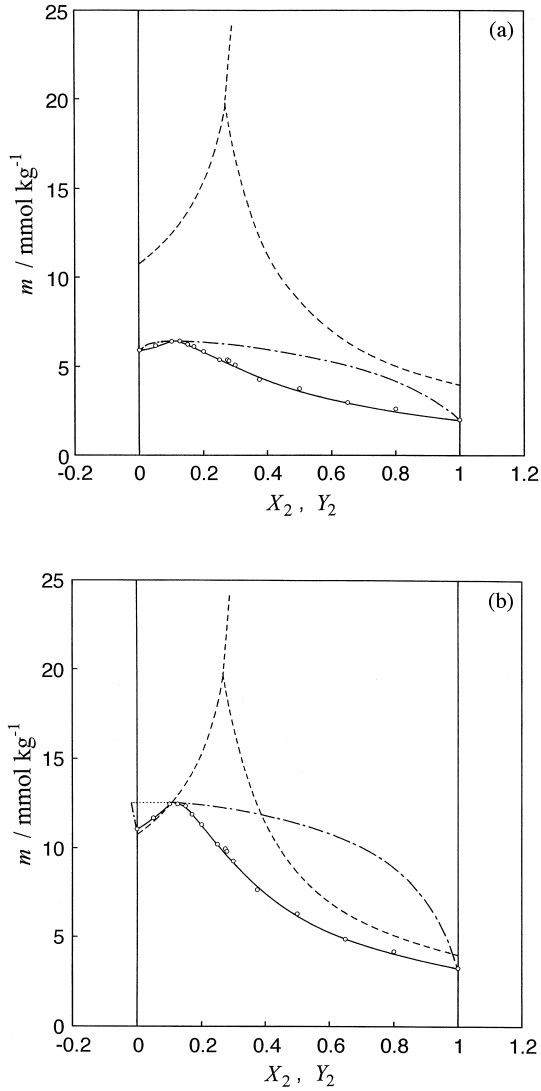


Figure 30 Phase diagram of adsorption of the C20OH–FC10OH system: (a) $\gamma = 45 \text{ mN m}^{-1}$, (b) 42.1, (c) 39, (d) 37, (e) 35; (—) m vs X_2 , (---) m vs Y_2 , (.....) m^{eq} vs X_2 .

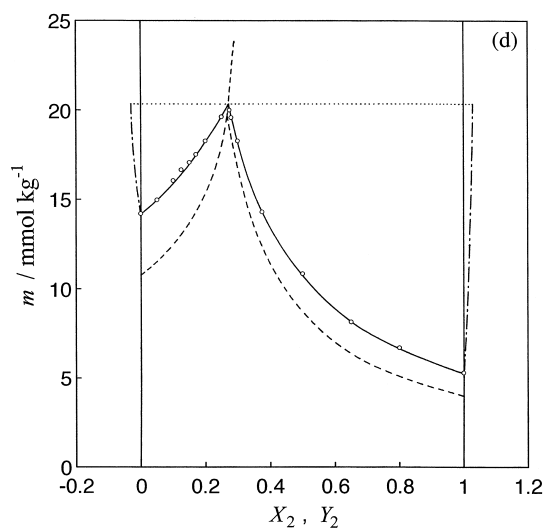
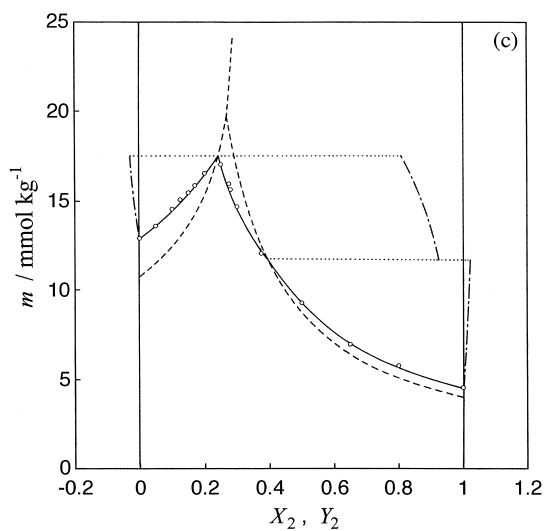


Figure 30 Continued.

As the interfacial tension decreases, the azeotropic point approaches gradually the m^{eq} vs X_2 curve and finally touches it at 42.1 mN m^{-1} as shown in Fig. 30(b). The m vs X_2 curve at lower X_2 sits in the condensed region (B in Fig. 29) and the Y_2 values evaluated are nearly zero or even very slightly negative.

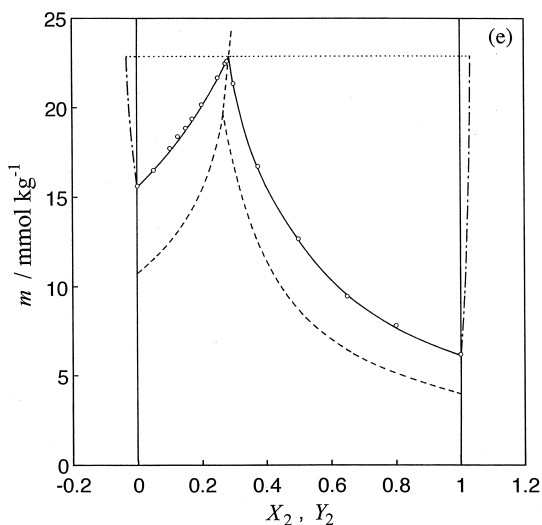


Figure 30 Continued.

This finding shows clearly that the condensed film in the B region is constructed only from C20OH molecules and thus FC10OH molecules are expelled from the interfacial region, which forms a striking contrast with the expanded film.

At 39 mN m^{-1} given in Fig. 30(c), the m vs X_2 curve is divided into three parts by the two break points on the m^{eq} vs X_2 curve. At the larger X_2 (region C), the condensed film of FC10OH appears and the mole fraction Y_2 is almost equal to unity: the condensed film is composed of only FC10OH molecules and C20OH molecules are expelled from the adsorbed film. This is a totally opposite situation to the one at the smaller X_2 (region B). At the intermediate X_2 (region C), the adsorbed film is in the expanded state and the Y_2 value changes with X_2 . At the interfacial tensions below 37 mN m^{-1} given in Figs 30(d) and (e), the adsorbed film is in a condensed state in a whole composition range and the PDA shows the heteroazeotrope. Thus the adsorbed film is constructed from only C20OH molecules below and from only FC10OH molecules above the bulk mole fraction at the azeotropic point.

Taking note of these PDAs, we draw a conclusion on the second break points observed on the γ vs m curves at $X_2 = 0.275$

and 0.280 (curves 9 and 10 in Fig. 26) as follows. Looking at the PDAs in Figs 30(d) and (e), it is seen that the heteroazeotropic point sit below $X_2=0.275$ at 37 mN m^{-1} and above $X_2=0.280$ at 35 mN m^{-1} . Therefore it is said that the adsorbed films at these X_2 at a concentration between the first and second break points is composed of only FC10OH molecules and those above the second break point is composed of only C20OH molecules. This is totally consistent with our conclusion that the second break point corresponds to the phase transition from the FC10OH condensed state to the C20OH condensed state.

The positive azeotrope and the complete immiscibility of C20OH and FC10OH molecules in the adsorbed film come from the rather weak interaction between hydrocarbon and fluorocarbon chains. The excess Gibbs free energy of adsorption at different interfacial tensions is given in Fig. 31: the g^{HE} values are positive at all Y_2 . Therefore it is said that the mutual interaction between C20OH and FC10OH molecules in the adsorbed film is very weak compared to that between the

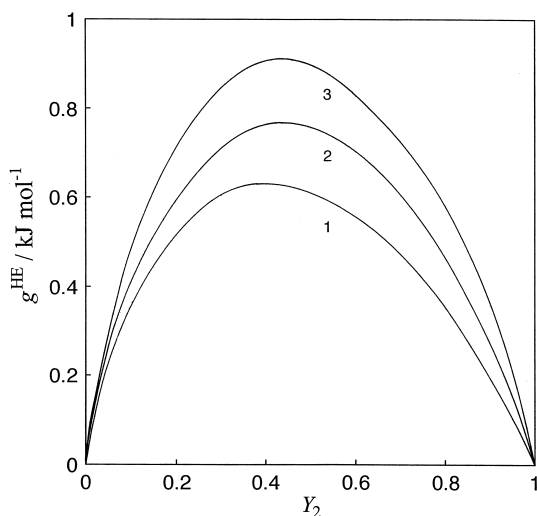


Figure 31 Excess Gibbs free energy of adsorption vs mole fraction in the adsorbed film of the C20OH-FC10OH system: (1) $\gamma=47 \text{ mN m}^{-1}$, (2) 45, (3) 43.

same type. It should be noted that the g^{HE} value is much larger than that of nonionic fluorocarbon and hydrocarbon surfactant mixture given in Fig. 6. Furthermore the excess area in the adsorbed film calculated by using Eq. (44) was positive and its maximum value is about 0.1 nm^2 [10]. Judging from the fact that the cross-sectional areas of hydrocarbon and fluorocarbon chains are about 0.2 and 0.3 nm^2 , respectively, and the maximum value of the corresponding excess area of the C10E4 and FC7E4 mixture is only about 0.025 nm^2 , we realize that the mixing of C20OH and FC10OH molecules in the adsorbed film causes a great increase in the mean area per molecule. This supports strongly the weak mutual interaction between the hydrocarbon and fluorocarbon alcohols.

V. CONCLUSION

The thermodynamic equations were abstracted from our systematic studies on binary surfactant mixtures to shed light on their miscibility in the adsorbed film and micelle. The representative systems of nonionic–nonionic, ionic–nonionic, ionic–ionic with and without common ions were examined by applying the equations. It was clearly shown that the dissociation of ionic surfactants should be taken into account in the definition of the concentration variables and then in the thermodynamic equations and that the resulting equations were different from each other, depending on the combination of binary surfactants. Furthermore the criterion of the ideal mixing in the phase diagram of adsorption and that of micelle formation were proposed and examined to elucidate the deviation from the ideal mixing in terms of the activity coefficients and excess Gibbs free energy.

The methods for ordinary micelles and adsorbed films were further extended to the spontaneous vesicle formation of cationic–anionic surfactant mixture and the phase transition of hydrocarbon and fluorocarbon alcohol mixtures at the oil/water interface, respectively. In the former, it was demonstrated that the phase diagram suggested from the simple model is consistent with that predicted from the surface

tension measurements and also with the visual and microscope observations. In the latter, the phase diagram of adsorption manifested that the miscibility of the alcohols were drastically changed by the phase transition in the adsorbed film.

REFERENCES

1. For example, *Curr. Opinion in Colloid Interface Sci.* **1**: 1 (1996); **2**: 243 (1997); **3**: 285 (1998); **4**: 175 (1999); **5**: **6**: 93 (2001).
2. J. R. Lu, R. K. Thomas, and J. Penfold, *Adv. Colloid Interface Sci.* **84**: 143 (2000).
3. D. N. Rubingh, *Solution Chemistry of Surfactants* (K. L. Mittal, ed.), Plenum Press, New York (1979), p.337.
4. D. Blankschtein, A. Shiloach, and N. Zoeller, *Curr. Opinion in Coll. Interface Sci.* **2**: 456 (1997).
5. I. Reif, M. Mulqueen, and D. Blankschtein, *Langmuir* **17**: 5801 (2001) (and references cited therein).
6. J. D. Hines, *Curr. Opinion in Coll. Interface Sci.* **6**: 350 (2001).
7. K. Motomura and M. Aratono, *Mixed Surfactant Systems* (K. Ogino and M. Abe, eds), *Surfactant Science Ser. 46*, Marcel Dekker, New York (1992), p. 99.
8. M. Villeneuve, S. Kaneshina, T. Imae, and M. Aratono, *Langmuir* **15**: 2029 (1999).
9. T. Takiue, T. Matsuo, N. Ikeda, K. Motomura, and M. Aratono, *J. Phys. Chem.* **102**: 4906 (1998).
10. T. Takiue, T. Matsuo, N. Ikeda, K. Motomura, and M. Aratono, *J. Phys. Chem.* **102**: 5840 (1998).
11. M. Aratono, M. Villeneuve, T. Takiue, N. Ikeda, and H. Iyota, *J. Colloid Interface Sci.* **200**: 161 (1998).
12. K. Motomura, *J. Colloid Interface Sci.* **64**: 348 (1972).
13. K. Motomura, S. Iwanaga, M. Yamanaka, M. Aratono, and R. Matuura, *J. Colloid Interface Sci.* **86**: 151 (1982).
14. K. Motomura, M. Yamanaka, and M. Aratono, *Colloid Polym.* **262**: 948 (1984).

15. J. H. Clint, *J. Chem. Soc. Faraday I* **71**: 1327 (1975).
16. B. T. Ingram, *Colloid Polymer Sci.* **258**: 191 (1980).
17. M. Aratono, T. Kanda, and K. Motomura, *Langmuir* **6**: 843 (1990).
18. Y. J. Nikas, S. Puvvada, and D. Blankschtein, *Langmuir* **8**: 2680 (1992).
19. N. Funasaki, *Mixed Surfactant Systems* (K. Ogino and M. Abe, eds), *Surfactant Science Ser. 46*, Marcel Dekker, New York (1992), p.145 (and references cited therein).
20. A. Ohta, H. Matsubara, N. Ikeda, and M. Aratono, *Colloids Surfaces A*, **183–185**: 403 (2001).
21. H. Matsuki, S. Kaneshina, N. Ikeda, M. Aratono, and K. Motomura, *J. Colloid Interface Sci.* **150**: 331 (1992).
22. J. C. Ravey, A. Gherbi, and M. Stébé, *Prog. Colloid Polym. Sci.* **79**: 272 (1989).
23. M. Villeneuve, T. Nomura, H. Matsuki, S. Kaneshina, and M. Aratono, *J. Colloid Interface Sci.* **234**: 127 (2001).
24. A. Shiloach, and D. Blankschtein, *Langmuir* **14**: 1618 (1998).
25. J. D. Hines, R. K. Thomas, P. R. Garrett, G. K. Rennie, and J. Penfold, *J. Phys. Chem. B* **101**: 9215 (1998).
26. V. M. Garamus, *Chem. Phys. Lett.* **290**: 251 (1998).
27. H. Matsubara, A. Ohta, M. Kameda, M. Villeneuve, N. Ikeda, and M. Aratono, *Langmuir* **15**: 5496 (1999).
28. H. Matsubara, A. Ohta, M. Kameda, M. Villeneuve, N. Ikeda, and M. Aratono, *Langmuir* **16**: 7589 (2000).
29. H. Matsubara, S. Muroi, M. Kameda, N. Ikeda, A. Ohta, and M. Aratono, *Langmuir* **17**: 7752 (2001).
30. M. Villeneuve, H. Sakamoto, H. Minamizawa, N. Ikeda, K. Motomura, and M. Aratono, *J. Colloid Interface Sci.* **194**: 301 (1997).
31. K. Motomura, H. Matsukiyo, and M. Aratono, In *Phenomena in Mixed Surfactant Systems* (J. F. Scamehorn, ed.), *ACS Symposium 311*, American Chemical Society, Washington, D.C. (1986), p. 163.

32. K. Motomura, N. Ando, H. Matsuki, and M. Aratono, *J. Colloid Interface Sci.* **139**: 188 (1990).
33. H. Matsuki, N. Ando, M. Aratono, and K. Motomura, *Bull. Chem. Soc. Jpn.* **62**: 2507 (1989).
34. C. Tondre, and C. Caillet, *Adv. Colloid Interface Sci.* **93**: 115 (2001).
35. T. Takiue, T. Fukuta, H. Matsubara, N. Ikeda, and M. Aratono, *J. Phys. Chem. B.* **105**: 789–795 (2001). [This is the latest paper and No. 8 of the series on the thermodynamic study on phase transition in adsorbed film of fluoroalkanol at the hexane/water interface. Other papers of this series are cited in this article.]
36. Z. Zhang, D. M. Mitrinovic, A. M. Williams, Z. Huang, and M. L. Schlossman, *J. Chem. Phys.* **110**: 7421 (1999).

Micro-Phase Separation in Two-Dimensional Amphiphile Systems

TEIJI KATO and KEN-ICHI IIMURA

Faculty of Engineering, Utsunomiya University,
Utsunomiya, Japan

SYNOPSIS

Micro-phase separation in binary mixed Langmuir monolayers of immiscible amphiphiles is an interesting phenomenon. In this chapter, we mainly discuss two subjects in relation to this phenomenon. The first one is the mechanism of micro-phase separation in μm size region and control of the size and shape of two-dimensional condensed phase domains. The second one is formation of surface micelles in the monolayers of partially fluorinated long-chain acids and micro-phase separation in their mixed monolayers in nm size region.